The Characterisation of Polymer Dispersed Liquid Crystal (PDLC) Films

AN INVESTIGATION INTO HOW THE MORPHOLOGY OF THE POLYMERIC BINDER AND DOPING WITH DICHROIC DYES AFFECT THE ELECTRO-OPTICAL PROPERTIES OF PDLC FILMS

E. J. Williams
St. Cuthbert's Society, University of Durham

4th Year MSci Physics Research Project 2001/2002
Supervisors: Professor D. Bloor
Dr. L.-O. Pålsson

In Association With SONY

CONTENTS

1. ABSTRACT

The aim of this project is to investigate how the morphology of the polymeric binder (i.e. the size, shape and number density of LC droplets) in a polymer dispersed liquid crystal (PDLC) film is affected by the concentration of LC in the polymer, the intensity of light used to cured the monomer, and the temperature of the PDLC during curing, as well as the addition of dye dopants. This has been achieved by examining a wide variety of electro-optical properties, such as absorption and transmission contrast ratios (with the aim of deducing any correlation between them, if one exists), viewing angle dependence measurements, switching speed times, switching voltages, as well as hysteresis. Polarised microscopy has been used to directly observe the form of the polymeric matrix, but a more powerful imaging technique has been deemed necessary. The Merck LCs, BL001 (in conjunction with the ultra-violet-light-curable monomer, NOA 65) and BL024 (in tandem with visible-light-curable monomers, NOA 72 and NOA 76), have been investigated, in tandem with a suite of dichroic dyes consisting of 17 IRL (New Zealand) dyes and 4 Niopik (Russian) dyes, of a variety of colours. It has been found that it is difficult to obtain uniform polymerisation by using the monomers that are cured in the visible wavelength range, hence specialisation in UV curing has been undertaken. 16 of the IRL dyes have been found to be insoluble in BL001, but the remaining dyes have been noted to exhibit interesting and useful properties. An attempt has been made to create a black dye using different combinations of the Russian dyes, by creating uniform absorption at all wavelengths in the visible range. All films have been fabricated by means of the polymerisation- or photopolymerisation-induced phase separation (PIPS) process, which has been observed to be conducive to good adjustment of the droplet diameters. The feasibility of using plastic substrates to create flexible displays has also been probed, with particular emphasis on the mechanical stability. The work is carried out in association with Sony, in their efforts to create "electronic paper".

2. INTRODUCTION

2.1 What is a Liquid Crystal?

A *liquid crystal* (LC) is a material that can flow like an isotropic liquid, yet retain some kind of orientational or positional order of its molecules, analogous to a crystalline solid.[1] These special properties are manifested in the liquid crystalline *mesophase*, which exists only within a certain temperature range (for *thermotropic* LCs), or at a critical concentration (for *lyotropic* LCs);[2] only thermotropic LCs have technological applications, hence all subsequent discussion will be devoted to this type. At temperatures below the mesophase, the material becomes a crystalline solid, and above, an isotropic liquid. Within the mesophase, all the molecules' long axes tend to line up along a certain direction known as the *director*, $\hat{n}$, usually designated by the boundaries of the sample (for instance, the director in a thin film of LC between glass substrates will align in the plane of the substrates); this is illustrated in **Fig.1**.[1] This phenomenon stems from the rod-like or elliptical shape of the LC molecules,[2] and their constant thermal motion - minimisation of the free energy of the system is reached only when the molecules are aligned with each other. When there exists only long-range orientational order of the molecules, with no long-range positional order, the LC is termed *nematic*.[2]

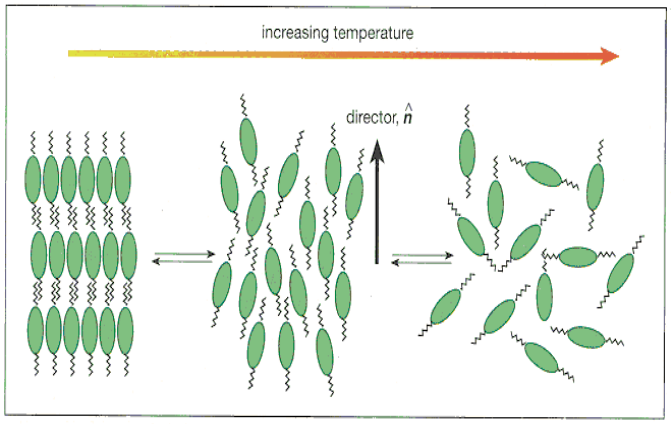

Fig.1: Scheme showing the three possible phases of a thermotropic LC – a crystalline solid at low temperatures, an isotropic liquid at high temperatures, and a material with intermediate properties when the LC is in its mesophase, within a certain temperature range. Note that these are nematic LC molecules, since there is no positional order of molecules in the mesophase

When the molecules also exhibit a long-range positional order, they are named *smectic* LCs.[2] The third and final type of LC is called *cholesteric* or *chiral nematic*, which is similar to nematic LCs, only now the director sweeps out a helix upon passage through the sample.[2] The utilisation of the nematic class of LC in commercial applications is considerably more widespread than use of the other two classes, thus all subsequent discussion will concentrate on nematics.

In the LC mesophase, a nematic liquid crystal (NLC) is *optically anisotropic*, or, in other words, it possesses *birefringence*, $\Delta n = n_e - n_o = n_{//} - n_{\perp}$ (where $n_e = n_{//}$ and $n_o = n_{\perp}$ are its ***extraordinary*** and ***ordinary*** refractive indices, respectively), which is typically positive for a LC.[1] The notation, $n_{//}$ and $n_{\perp}$, can be used since n_e and n_o represent the refractive indices of an aligned sample of LC molecules presented to an incident beam of light, when its polarisation vector is, respectively, parallel and perpendicular to the long molecular axes. Since the *optic axis* of a medium is

defined as being the direction along which a beam of light (of arbitrary polarisation) experiences only the ordinary refractive index of that medium, the optic axis of a sample of LC lies along the director.

In addition to an optical anisotropy, LCs also possess a *dielectric anisotropy*, $\Delta\varepsilon=\varepsilon_{//}-\varepsilon_{\perp}$, where $\varepsilon_{//}$ and $\varepsilon_{\perp}$ denote the *dielectric constants* (or *relative permittivities*) as measured between electrodes which are parallel and orthogonal to the long molecular axes of the LC molecules, respectively.[1] This anisotropy arises by virtue of permanent and, more importantly, induced electric dipole moments in the molecules, stemming from an uneven distribution of charge across each molecule, and greater electronegativity at one end than the other; the molecules are, however, net electrically neutral.[3] For positive $\Delta\varepsilon$ (which is predominantly the case for LCs[1]), the long molecular axis of a LC molecule will thus respond more readily to an applied electric field than the short axis, hence LC molecules reorient to align their long molecular axes (and hence, optic axis) with the applied field, provided it is sufficiently strong to overcome the *anchoring energy* created by the boundaries of the sample. Weak fields will thus allow only partial reorientation with the field, and the removal of any applied field tends to result in the LC director relaxing back to resume its original orientation. LC molecules may also respond to very large magnetic fields via their minute magnetic dipoles, but the effect is insignificant in comparison to the influence of electric fields.[2] Their ability to electrically control the refractive index presented to an incident beam of light bestows LC molecules with considerable practical utility.

2.2 Conventional Liquid Crystal Display (LCD) Technology

In 1971, the broad application of LCDs became feasible when the *twisted nematic* (TN) cell was invented by Schadt and Helfrich,[4] a construction which would ultimately become the workhorse of the portable display industry; this is shown in **Fig.2**.[1] Here, a NLC is sandwiched between two transparent glass or rigid plastic substrates, which each have a very thin (~0.1 microns) coating of *indium tin oxide* (ITO) on their inside faces to form transparent electrodes, allowing a large electric field (~10^6 Vm^{-1}) to be placed across the film (typically 10 microns thick[4]) under application of a modest voltage (~10 V).

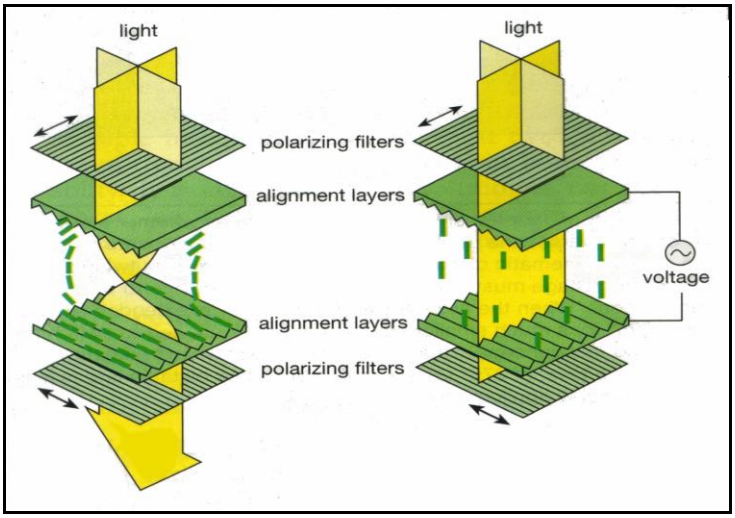

Fig.2: Scheme of the twisted nematic (TN) cell in the OFF and ON states

The ITO is coated with a thin layer of directionally rubbed polyimide, where the rubbing direction on one of the substrates is perpendicular to that on the other; in tandem with alignment in the plane of the substrates, the nematic director now also aligns with these rubbing directions, with the result that the director rotates uniformly through 90° from one substrate to the other.[4] In this form, the LC molecules serve to "waveguide" the polarisation of incident light, rotating the plane of polarisation through a right angle as it propagates through the film.[1,2] Application of a sufficiently large electric field will reorient the LC molecules with the field (normal to the substrates), destroying the helical structure; hence, the LC molecules cease to be optically active, and their sole influence on a normally incident beam of light is caused by n_o. Thus, placement of this structure between crossed polarisers creates the TN cell, which allows almost full transmission of normally incident light in the absence of an electric field (the *OFF state*), but becomes completely black and opaque (for perfect polarisers) when a field is applied (the *ON state*), since the second polariser's transmission axis is now orthogonal to the plane of polarisation of propagating light. Placement of a mirror beneath the second polariser forms the traditional reflective LCDs familiar from digital watches and calculator displays, where there is a TN cell at each pixel, or at each segment of a seven-segment display.

2.2.1 Problems with Conventional LCD Technology

Problems inherent with this technology stem from the use of polarisers: 50% of the incident (unpolarised) light is absorbed by the first polariser, resulting in marred image brightness. Also, light with increasingly oblique angles of incidence will have poorer and poorer rotation of its plane of polarisation upon passage through the (OFF state) LC, hence more and more light will be absorbed by the second polariser. This results in a dark OFF state when a conventional LCD is viewed at large angles, severely impairing its picture quality. Standard LCDs are also susceptible to pressure and, as such, offer no mechanical stability – fabrication of large displays is infeasible, since it is highly impractical to stringently maintain the film thickness of several microns over large areas.

2.3 What is a Polymer Dispersed Liquid Crystal (PDLC) Film?

Both fundamental aspects of science and practical applications have led to intensive study of LC-polymer composites.[5] Invented in 1986 by Doane *et al.*,[6] *a polymer dispersed liquid crystal* (PDLC) film is an electrically switchable composite device, consisting of a thin layer (typically 5 to 30 microns) of micron-sized LC droplets (predominantly utilising the nematic phase, though cholesteric and smectic phases can also be deployed[7]) dispersed in a polymeric matrix, which is sandwiched between two transparent, ITO-coated glass or plastic substrates.[5] Spheroidal or ellisoidal nematic droplets tend to adopt the bipolar tangential configuration, depicted in **Figs.3(a)** and **(b)**[8,9] (in the absence and presence of an electric field, respectively), where the droplet director is defined as the line joining the two poles, since this is the average direction of the long molecular axes of the LC molecules in the droplet.

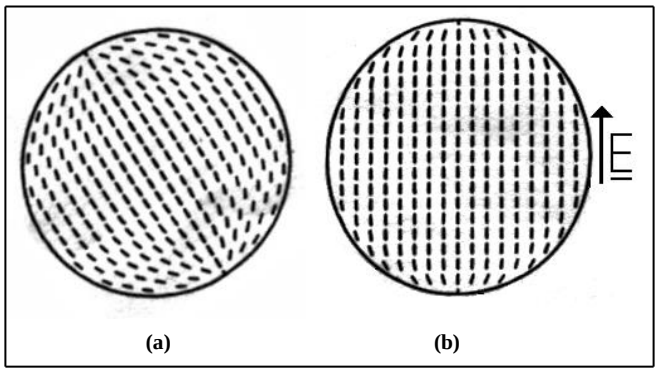

Fig.3: Scheme of the bipolar tangential configuration adopted by NLC molecules in a spheroidal or ellipsoidal droplet, in **(a)** the absence of an electric field, and in **(b)** the presence of an electric field. The lines represent the long molecular axes of the NLC molecules

In reality, perfectly spherical droplets do not exist, and it is the presence of deformities that leads to a preferred direction for the droplet director – for an ellipsoidal droplet, it is energetically favourable for the director to lie along its semi-major axis. The presence of an electric field, if sufficiently large, causes reorientation of the LC molecules with the field, except at the surface of the droplet where the anchoring energy will always be too large to allow total reorientation. In a PDLC film, in the absence of an applied field (the OFF state), the droplet directors are randomly oriented, and there exists virtually no correlation between the directors of neighbouring droplets;[7] this is depicted in **Fig.4**.[8]

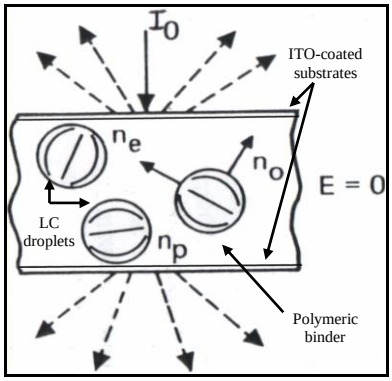

Fig.4: Scheme of PDLC device operation in the OFF state, demonstrating the randomly oriented uniaxial birefringent LC droplets, dispersed in a polymeric matrix, scattering the incident light, I_0. It should be noted that light may encounter many droplets upon passage from one substrate to the next, as opposed to the ~2 illustrated here

The director defines the optic axis of a droplet,[5] hence it is along this direction that light traversing a droplet will experience only the ordinary refractive index, n_o, of the LC. Light propagating perpendicular to this will "see" only the extraordinary index of refraction, n_e, if it is polarised parallel to the director, or n_o if it is polarised perpendicular. Unpolarised light which is obliquely incident will experience a combination of these two refractive indices; thus, by virtue of the arbitrary orientation of droplet directors, light incident on a film will "see" nematic droplets of mean refractive index:[7]

$$\overline{n} \simeq \frac{n_o + n_e}{2} \qquad \textbf{(1)}$$

embedded in a polymeric matrix of refractive index, n_p. With an appropriate selection of LC and polymer, the mismatch between $\overline{n}$ and n_p can be maximised, and, provided the diameters of the droplets are of the order of the wavelength of incident light, these droplets become scattering particles.[5] For a film which is 10 microns thick, a beam of light may encounter ~10 droplets whilst traversing the film, leading to extensive scattering. Hence, the OFF state has a translucent

white appearance (or even completely opaque for sufficient refractive index mismatch, optimum droplet size, ample number density of LC droplets and large film thickness), when irradiated with ambient light.[6,8]

All the droplets' directors will align themselves with the field when a sufficiently large voltage (termed the *saturation voltage*) is applied across the substrates (i.e. when the PDLC is in the ON state), hence the optic axes of all droplets will be normal to the substrates – consequently, light normally incident on the film will "see" droplets with a refractive index of n_o. Thus, if n_p can be made to match n_o, normally incident light will experience negligible index mismatching as it propagates through the film, resulting in the scattering OFF state being eliminated in favour of a transparent ON state; this is depicted in **Fig.5**.[8]

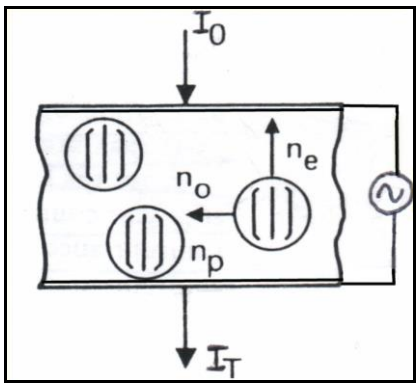

Fig.5: Scheme of PDLC device operation in the ON state, demonstrating how droplet directors align with an applied field. Provided $n_p=n_o$, the scattering will cease, and most of the incident light will be transmitted undeviated.

The point at which the LC molecules only just begin to reorient with the field is referred to as the *Freedericksz* transistion.[3] Increasing the field slightly from this point will achieve a scattering state which has 10% of the *transmission* of the film in the ON state (i.e. with the OFF state being defined as having 0% transmission), and the p.d. at which this occurs is termed the *threshold voltage*. Increasing the p.d. to lie in between the threshold and saturation voltages will produce an intermediate scattering state – hence, a PDLC cell can be deemed to exhibit *electrically controllable scattering*. At increasing angles of incidence, however, unpolarised light will be more and more influenced by n_e, and a semi-scattering state will remain, creating an inferior ON state at larger and larger viewing angles, exacerbated by the increased optical path length; the effective refractive index presented by the aligned molecules to the component of the impinging beam polarised in the plane of incidence is governed by **(2)** below, with θ being the angle between the incident beam and the normal to the substrates.[10]

$$n_{eff} = \frac{n_o \cdot n_e}{\sqrt{n_o^2 \sin^2\theta + n_e^2 \cos^2\theta}} \qquad \textbf{(2)}$$

The component of incident light which is polarised orthogonal to the plane of incidence experiences only the ordinary refractive index, independent of θ, so the scattering of this component will be the same as at normal incidence (i.e. very small, if $n_p \approx n_o$). Thus, if the ON state possesses high transparency at normal incidence with directional illumination, it should remain high when illuminated and viewed at angles at least as large as 50°.[10] If not, this could be alleviated by decreasing the birefringence, but this has the undesirable side effect of diminishing the OFF state opacity.

A mitigating factor is that there will be appreciable refraction at the air-glass or air-plastic interface, decreasing the angle of incidence of light entering the polymer binder. It can be deduced that for θ=45°, and in the limit of small Δn, n_{eff} from **(2)** approaches $\bar{n}$ of **(1)**, as would be expected. In addition to desiring that scattering in the ON state is minimised for light at all angles of incidence, good viewing angle dependence is also hinged upon attaining uniform scattering at all angles of transmission, so that a pixel can be viewed from any direction with equal clarity.

2.3.1 Doping PDLCs with Dichroic Dyes (The Guest-Host Effect)

If PDLCs are to be used for display applications, it is insufficient to have merely a milky white, opaque OFF state. *Dichroic dyes* (whose molecules' absorption spectrum is a function of the molecular orientation with respect to the polarisation of the incident light) may be utilised as dopants ("*guest*") in the LC ("*host*"), from which arises the so-called *guest-host effect*.[11] Here, the dye molecules interact with the LC molecules by means of van der Waals forces, hence the reorientation of the LC molecules in an applied field also leads to reorientation of the dye molecules, and this process is facilitated if the dye molecules are dipolar (i.e. if they possess permanent or, to a much lesser degree, induced electric dipoles), where faster switching speeds may be observed (or slower due to the increased viscosity of the mixture in the droplets). Thus, electrically controlled light absorption results, with the goal of creating a highly coloured OFF state due to most of the molecular axes of maximum absorption being aligned parallel to the substrates, and a transparent ON state via most being reoriented normal to the substrates by the LC molecules; however, this utopian scenario can never be fully realised due to the curvature of the LC droplet-polymer interface meaning that finite absorption will always be observed in the ON state, because the effect of the dye molecular axis of maximum absorption can never be truly nullified. It is of paramount importance to ensure that any dye dopant is fully dissolved in the LC before adding the material which forms the solidified polymer, since any residual dye may become trapped in the polymeric matrix, producing a permanently coloured ON state. The dye may also lead to a marred birefringence, but conversely the reverse may be true, enhancing the scattering properties.[12] Absorption in the OFF state is boosted by the increased optical path length, due to the multiple scattering of light traversing the film, resulting in a higher probability of dye absorption.[13,14] Moreover, if the afore-mentioned increase in the LC mixture's viscosity is not too large, a reduction in the switching voltages may also be observed.[12]

2.3.2 The Benefits and Applications of PDLC Technology

PDLC technology, with the inclusion of coloured dyes, renders the use of polarisers redundant, resulting in the auspicious consequence that 50% of the incident (unpolarised) light is no longer wasted, leading to much brighter reflective displays, and a reduction in power consumption in the case of back-lit displays. While it is true to say that polarisers can be omitted in non-polymer-dispersed LCDs by employing dichroic dyes, there are doubts over the long-term chemical stability of such displays; dispersing the dye-doped LC in a polymeric binder is thought to alleviate this

problem. Despite remaining a bone of contention, the viewing angle dependence of a PDLC is far superior to that of a TN-LCD, and this also due to the omission of polarisers.

Although the anchoring energy (i.e. the energy which restores the LC director to its original orientation upon removal of an applied field) in a LC droplet is significantly smaller than in the thin LC layer employed in conventional LCDs (except in the case of highly ellipsoidal droplets), the fact that the LC domains in a PDLC are so small leads to the significantly faster *decay times* (i.e. the time required to reinstate the OFF state) witnessed in PDLC displays (whilst maintaining a *rise time* – the time elapsed in achieving a transparent ON state, upon application of the field – comparable to standard LCDs).[7]

PDLCs are intrinsically mechanically stable, which enables truly large displays (which are metres in diagonal) to be realised; this is because it is considerably easier to maintain a constant film thickness over large areas with PDLC technology, by virtue of the polymeric binder, and the demands on maintaining uniform film thickness are less stringent. Furthermore, the substrates can be made of *flexible* plastic, allowing flexible displays to be fabricated! Also, cell fabrication is facilitated since there is now no requirement for directionally-rubbed alignment layers, which are expensive to produce.

If the ambitious task of discovering, or creating, a dye which appears jet black (by exhibiting equally large absorbance across the entire visible wavelength spectrum) in a PDLC film could be fulfilled, large, wall-mountable, flexible TVs in the guise of PDLCs are a potentiality, which could be viewed outdoors in direct sunlight, and, indeed may solely utilise ambient light, dramatically decreasing power consumption. Already, PDLCs find applications in switchable privacy screens/variable transmission windows, light valves, amplitude modulators,[7] and temperature sensors,[10] as well as projection TVs,[7] where the excellent brightness and switching speeds are exploited.

2.4 The Formation of LC Droplets via Phase Separation

A *monomer/oligomer* (also often termed a *prepolymer* or *polymer precursor*) is a simple chemical unit which forms a *polymer* – a long chain of covalently-bonded atoms - when many are joined together.[3] The genesis of *phase separation* in a homogeneous mixture of LC and monomer is a reduction in the solubility of the LC material, and this is induced by one of three methods:[5,8]

(1) Evaporation of a solvent included in the mixture, called solvent-induced phase separation *(SIPS)*

(2) Cooling of a thermoplastic-LC melt, called thermally-induced phase separation *(TIPS)*

(3) Curing of the monomer, called polymerisation-induced phase separation *(PIPS)*

The latter method has emerged as the most popular, allowing a pre-fabricated LC cell (consisting of two ITO-coated substrates separated by a distance of several microns) to be *capillary filled* with the homogeneous LC/monomer mixture (by heating the cell to reduce the mixture's viscosity), then curing the glue-like monomer to form a solidified

polymer by exposing it to light of a specified wavelength leads to the precipitation of LC droplets. The curing rate and temperature of curing both have a profound impact on the finished morphology of the polymeric binder, in conjunction with the concentration of LC in the monomer; hence, all subsequent discussion will be based on the PIPS method. Upon preliminary formation of phase-separated LC droplets, which is a *molecular diffusion process*, larger droplets can form by continued *diffusion/nucleation* or by *coalescence* of several droplets to form one.[7] These processes are truly complex, dependent on many factors, some of which are interrelated.

In the absence of dye dopants, there is much evidence to suggest that phase separation occurs along, or below, a line in temperature-composition space,[15,16,17] as depicted by the circular-dotted line in **Fig.6**.[17] Prior to curing, the homogeneous LC/monomer mixture is isotropic (i.e. the orientation of individual LC molecules is randomly distributed) above this line, and phase-separated, nematic LC-rich droplets/domains in an isotropic, monomer-rich binder exist below it.[15] Initiation of polymerisation leads to an expansion of the polymeric matrix (i.e. an increase in its average molecular weight[16]), with the consequence of increasing the temperature of the phase-separation line; hence, the phase-separation line moves towards the top-left of **Fig.6**, as the extent of polymerisation increases. Thus, nucleation of LC domains can only proceed once polymerisation has progressed far enough such that the phase separation line temperature matches or surpasses the PDLC cure temperature.[15]

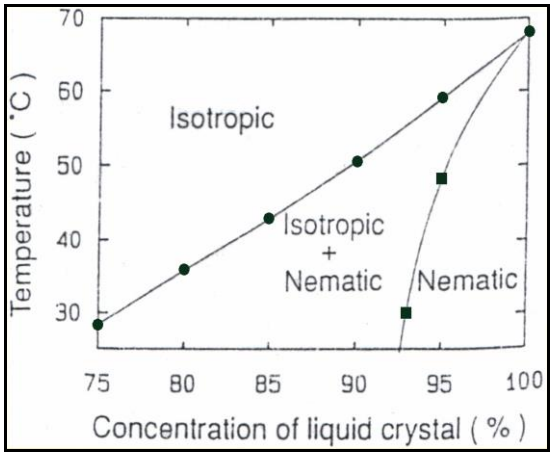

Fig.6: Typical phase space diagram for PDLC mixtures containing a high concentration of LC in a monomer, where the phase separation line is circular-dotted, which heads to the top-left of the diagram as polymerisation ensues. The numerical values will not be the same for different types of LC and monomer, but the form of the diagram should be retained.

For PDLC compositions and temperatures far above the phase separation line during curing, the matrix will be more polymerised at the onset of phase separation, limiting the nucleation time available to the droplets before sample solidification.[16] It can be deduced, by inspection of **Fig.6**, that higher temperatures of curing and lower LC concentrations are both conducive to smaller LC domains. Conversely, heating the LC/monomer mixture leads to a reduction in both of their viscosities, liberating and catalysing droplet coalescence, which drives the precipitation of larger droplets, which may become ellipsoidal in shape. Thus, both temperature and composition govern the extent of polymerisation at phase separation, after which the PDLC morphology is predominantly determined by four time-scales, which are the times required for:[15]

(1) Droplets to nucleate to their space-limited size via molecular diffusion

(2) Droplets to coalesce via movement of the polymeric matrix from between adjacent droplets

(3) Coalesced droplets to relax into spherical domains

(4) Sufficient solidification of the polymeric matrix to halt nucleation, coalescence, and relaxation of droplets

Unfortunately, the first three of these time-scales are intractable, since they too depend on temperature and composition.[15] However, it is found with combinations of *Merck's LC BL001* and *NOA (Norland Optical Adhesive) 65 monomer*, that it is only during the final 10% of polymerisation that the matrix becomes fixed, and once this has occurred, a fraction of the LC is permanently phase separated, with the rest remaining dissolved in the matrix.[18] Decreasing the curing light intensity reduces the rate of polymerisation, thus leading to increased fulfilment of the first three processes, which is conducive to larger droplets; a faster rate of curing stifles these processes, leading to smaller droplets. The PDLC morphology is fundamentally determined by the mechanism of nucleation (i.e. the first time-scale), but competition among these time scales can still play a major role.[15] Dye dopants in the mixture can have several effects, such as absorbing some of the light available for curing, leading to a slower rate of polymerisation, and hence larger droplets; conversely, the dye molecules may impede the droplet nucleation process, leading to smaller droplets. Ultimately, then, the final PDLC morphology is dependent on three crucial factors: the composition of PDLC mixture, the curing temperature and the curing intensity; the consensus is that the morphology at the microscopic level has a profound impact on the macroscopic electro-optical properties.[7,15,16]

2.5 Optical and Electro-Optical Properties

2.5.1 Light Scattering

The observed light scattering can be attributed to reflection and refraction at the curved LC/polymer interfaces, as well as birefringence (double refraction) throughout each droplet; a small proportion of the back-scattered light originates from reflection off the film substrates. There are three models to describe light scattering from PDLC films, each corresponding to a different diameter, D, of droplet and its relation to the wavelength of illumination, λ:[8,9]

(1) The *Rayleigh-Gans* approximation, for $D \ll \lambda$ and small Δn

(2) The *anomalous diffraction* approach, for $D \geq \lambda$

(3) The *geometrical optics* approach, for $D \gg \lambda$

Theories **(1)** and especially **(2)** are the most pertinent, both allowing an expression to be obtained for the total scattering or diffraction cross section, respectively, which are both found to scale inversely as a (different) power of wavelength;[8,9] hence, longer wavelengths scatter less. However, all three theories make a number of crude assumptions, the most inaccurate being the neglect of secondary scattering due to the film thickness and number density of droplets being so small – this is seldom the case in PDLCs.[9] Also, LC droplets are bounded by a thin transitional layer with

properties intermediate to the LC and polymeric matrix; furthermore, the optical properties of the cured polymer will differ slightly from a pure state due to the presence of LC (and/or dye dopants) dissolved therein.[8] It is therefore advisable, when endeavouring to select compatible LCs and monomers, to choose a monomer whose (polymerised) refractive index is slightly lower than the ordinary refractive index of the LC, to accommodate for the anticipated increase in the polymer's refractive index. For a given droplet size, the higher the LC concentration, the larger is the number density of droplets, leading to greater scattering, but higher concentrations may lead to more LC becoming permanently dissolved in the polymer, impairing the scattering.[8] The existence of back-scattering, while valuable from an applications perspective, further complicates the theory of the scattering process, as does the presence of deformations in the droplets.[7] The elucidation of a theory incorporating all the facets of real PDLC morphology does seem a formidable quest.[8] Consequently, there are conflicting reports over the optimum droplet size for scattering visible light, ranging from submicrometer,[5,6] to equal to visible wavelengths,[7] to micrometer,[8,13] to several microns.[19]

2.5.2 Viewing Angle Dependence

The light scattering properties of PDLC films give rise to diffraction-like patterns when the incident beam is collimated (e.g. a laser beam), and it is found that smaller droplets produce a broader central peak in intensity.[9] Thus, viewing angle dependence measurements (i.e. measurements of transmitted intensity for different angles of scattering) may be used to ascertain the average droplet size in a PDLC film. A general equation describing the intensity of light, $I(\theta)$, of wavelength, λ, scattered by particles of diameter, D, out to a small angle, θ, is:[20]

$$\ln\left(\frac{I(\theta)}{I(0)}\right) = -\left(\frac{2\pi D \sin\theta}{\sqrt{3}\lambda}\right)^2 \qquad \textbf{(3)}$$

Hence, a plot of the logarithm of the intensity of scattered light against minus the square of the sine of the scattering angle (i.e. a *Guinier* plot[20]) may be used to very roughly determine the mean droplet size, or at least allow a comparison of the droplet sizes of different PDLC films. **(3)** is only valid for $kD\sin\theta=1$, where k is the wavenumber of incident light; for the anticipated droplet size of ~1 μm, and for λ=633 nm, this condition is satisfied for $\theta=6°$.

2.5.3 Absorption/Absorbance

Using the simplifying assumption that the dye *absorbance* in a PDLC is independent of the film scattering, according to Beer's law, the *extinction coefficient*, γ, can be defined by:[13]

$$\gamma = \alpha + \beta \qquad \textbf{(4)}$$

where α denotes the *scattering coefficient*, and β the *absorption coefficient*. The absorbance of a PDLC originates solely from the dye content of the film, thus β can be defined as:[13]

$$\beta = \varepsilon c r \qquad \textbf{(5)}$$

where ε denotes the *dye extinction coefficient* [per molar (moles of dye per litre of medium) per cm] in a non-light-scattering film, c represents the dye concentration [molar], and r is the ratio of the distance travelled by the light to the film thickness (which is always larger than unity due to scattering). Analogous to Beer's law, the OFF-state *transmittance* (i.e. normalised transmitted intensity) of a PDLC film can be expressed as:[13]

$$T = \frac{I}{I_0} = \exp\left(-\gamma d\right) \tag{6}$$

where I_0 is the intensity of light transmitted by an empty LC cell, and I is that transmitted through a PDLC film of thickness, d [cm]. In the case where there is no scattering, $\gamma=\beta$, and **(6)** becomes:[13]

$$T = \exp\left(-\varepsilon c l\right) \tag{7}$$

where l is the *optical path length*. In the case of a cuvette, where l=1 cm, the quantity in the exponential defines the (negative) *absorption* (with units of *optical density*, *OD*), otherwise it is termed the (negative) absorbance (with arbitrary units). Both are denoted by A, and given by:[13]

$$A = \varepsilon c l = \ln\left(\frac{1}{T}\right) = \ln\left(\frac{I_0}{I}\right) \tag{8}$$

Both absorption and absorbance can be measured using an *absorption spectrometer*.

2.5.4 Ideal Dye Properties

For dichroic dyes to be suitable for use in PDLCs , they should possess the following properties:[14]

(1) Chemical and photochemical stability

(2) Non-ionic nature

(3) High solubility in the LC (but ideally low in monomer)

(4) Produce only small increase in the viscosity of the LC

(5) High order parameter

(6) High extinction coefficient

(7) High resistivity

(8) Highly dipolar

(9) Low absorption at UV wavelengths (if used in conjunction with UV-curable monomers)

(10) Low molecular weight

The *order parameter* of the dye, S, which describes how well the dye molecules align with the director of a liquid crystal (with a value of zero for complete disorder, and a value of unity for perfect order), is defined by:[7,19]

$$S = \frac{A_{\parallel} - A_{\perp}}{A_{\parallel} + 2A_{\perp}} \quad \textbf{(9)}$$

where $A_{\parallel}$ and $A_{\perp}$ denote the dye absorbances for light polarised linearly, respectively, parallel and perpendicular to the long molecular axes of the dye. These values are most easily determined from measurements on non-polymer-dispersed LCDs, using cells with alignment layers where the rubbing direction on one of the substrates is diametrically opposed to that on the other.

The solubility of the dye in LC (and in monomer) is expected to be a function of temperature, but any dye dissolved at higher temperatures is likely to precipitate out of solution at room temperature. The addition of dye beyond the solubility limit in the LC may result in the undesirable effect of dye aggregation, where clumps of dye form. Heating the LC/dye mixture once the monomer has been added may result in the dye molecules overcoming the van der Waals forces and becoming dissolved in the monomer, leading to a permanently coloured ON state upon curing. Criterion **(1)** is most likely to be unsatisfied in the case of plastic substrates, which allow photoreactions of dyes to take place under *aerobic* conditions (as opposed to glass cells which inhibit the diffusion of oxygen into the system, maintaining *anaerobic* conditions), which are shown to significantly impair the stability of dichroic dyes.[19]

2.5.5 Contrast Ratio

The hallmark of a "good" LCD is a high *contrast ratio* (CR), but unfortunately there are a plethora of different definitions of this quantity, making comparisons of the CRs of different displays measured using different methods rather misleading. For dye-doped PDLCs, the most suitable quantity is the OD (*optical density*) CR, which is defined as:

$$CR = \frac{A_{off}}{A_{on}} \quad \textbf{(10)}$$

where A_{off} is the absorbance of the film in the OFF state (measured at the wavelength of peak absorbance, λ_{max}), and A_{on} is that in the ON state. While a typical conventional LCD can muster OD CRs in excess of a hundred (where A_{off} and A_{on}, in this instance, represent the absorbances in the darkened and transparent states, respectively), PDLCs rarely surpass fifteen, due to the low absorbance in the OFF state. Indeed, in the case of a PDLC without the inclusion of dopants, "absorbance" is somewhat of a misnomer, because polymer and LC molecules absorb almost no visible light,[13] with the perceived absorbance actually originating from incident light being forward- and backward-scattered by the film, away from the detector. Correction for the absorbance/reflection due to the presence of the substrates is sometimes performed, and from the perspective of **(8)** this can be done by subtracting the absorbance of an empty glass cell from the numerator and denominator in **(10)**.

Another definition of contrast ratio is:[7,13]

$$CR = \frac{T_{on}}{T_{off}} \quad \textbf{(11)}$$

where T_{on} and T_{off} are the transmittances in the ON and OFF states, respectively. These quantities are best measured by using a laser to probe the PDLC, hence this type of CR is better suited to undoped PDLCs since it can only be measured at the laser's wavelength. From the perspective of **(6)**, these CRs are automatically corrected for the absorbance/reflection of light from the substrates. The distance from the PDLC to the detector (in addition to the detector's acceptor angle) will have a profound effect on both types of CR, with larger distances meaning that more light is scattered away from the detector in the OFF state (and the ON state, to a much lesser degree), leading to larger CRs.

2.5.6 The Use of an Alternating Electric Field

A PDLC is essentially a capacitor (capacitance, C); applying a static voltage causes charge, Q, to gradually build up on the electrodes (until $Q=VC$), so that a permanent field remains until the cell is discharged. Hence, an alternating field must be utilised. If a sufficiently high frequency is used (i.e. larger than the reciprocal of the decay time), the cell will switch to the ON state and will not have time to switch OFF before the beginning of the next cycle; hence, the nematic directors will oscillate about an axis approximately perpendicular to the substrates, with the consequence that the cell will appear to be ON. If too high a frequency is applied (i.e. much larger than the reciprocal of the rise time), the cell will exhibit negligible switching before the polarity is reversed, so the nematic directors will oscillate about an axis approximately parallel to the substrates, with the consequence that the cell will appear to be OFF. The optimum frequency is of the order of the reciprocal of the characteristic rise times, but up to two orders of magnitude higher may also be adequate, depending upon the size of the applied field.

This matter is further complicated by the frequency dependence of the dielectric and resistive properties of the LC/polymer/dye media as a whole, which has a bearing on how much shielding is presented to an applied external field, and thus how large the field is inside a droplet; at high frequency (i.e. 1 to 10 kHz), the shielding is governed by the dielectric constants of the polymer, ε_p, and LC, ε_{LC} (which, of course, is dependent upon the size of the field in the LC droplets, and the average quiescent orientation of the droplet directors), where the electric field inside a droplet, E_{LC}, is given by:[8]

$$E_{LC} = E_p \frac{3\varepsilon_p}{2\varepsilon_p + \varepsilon_{LC}} \quad \textbf{(12)}$$

where E_p is the field in the polymer. At lower frequencies, E_{LC} possesses a dependence on the conductivities of the LC and polymer, as opposed to the dielectric constants;[8] also **(12)** will take on a different form when dye dopants enter the fray. Nevertheless, it does elucidate the fact that a polymer with a high dielectric constant is conducive to a lower switching voltage.

2.5.6 Switching Voltages

The saturation voltage, V_{sat}, is difficult to measure accurately, hence a more useful parameter is V_{90}, which is the applied voltage required to achieve 90% of the maximum transmission (where the OFF state is 0%). The threshold voltage, V_{th}, can be denoted by V_{10}, from its definition of being the applied voltage required to achieve 10% of its maximum transmission (above the OFF state). V_{10} and V_{90} both have the following dependence for non-dye-doped films, at high frequency:[5,8,15,16]

$$V_{10} \sim V_{90} \sim \frac{d}{a}\left(\frac{2\varepsilon_p+\varepsilon_{LC}}{\varepsilon_p}\right)\left(\frac{K(l^2-1)}{\Delta\varepsilon}\right)^{\frac{1}{2}} \qquad \textbf{(13)}$$

where a and b are, respectively, the lengths of the *semi-major* and *semi-minor* axes of the droplets ($a=b$ for spherical droplets), $l=a/b$ is the *aspect ratio* of the droplets, K is the *effective deformation elastic constant* of the LC, and $\Delta\varepsilon$ is the dielectric anisotropy of the LC. It can be seen from **(13)** that thicker LC cells are conducive to a higher switching voltage, so there is an inevitable trade-off between low driving voltage and high contrast. A high dielectric anisotropy is thus desirable, and this may be increased via the inclusion of dye dopants. It is found that a higher concentration of LC also lowers the switching voltages,[8] though this is not apparent from **(13)**. The equation only applies to ellipsoidal droplets, since for perfectly spherical LC domains (i.e. where l=1) it predicts that a PDLC film will switch ON with no applied field! This implies that a complete equation for V_{10} and V_{90} requires an additional term that is independent of the morphology.[15]

Compared to similar equations for conventional LCDs, the switching voltages are a factor of at least $\sim d/a \sim 10$ larger,[5] which is an inherent downfall of PDLC displays. This possibly makes them unsuitable for *active-matrix-addressed displays* (where a TFT – *thin film transistor* – is fabricated at each pixel, to accurately control the voltage across it until it is next addressed), since TFTs can only hold voltages up to 13.5 $V_{p\text{-}p}$. Also, for multiplexed displays (i.e. displays which deploy rows of electrodes on one substrate, and columns on the other, so that each pixel – where the electrodes cross – can be individually addressed) it is necessary to have only a small difference between V_{10} and V_{90} (i.e. a large gradient in the *electro-optical characteristic*, which is traditionally the graph of transmittance versus applied voltage).[21] From **(13)**, it is not apparent how the difference between V_{10} and V_{90} arises, but it is generally observed that PDLCs have shallower electro-optical characteristics than conventional LCDs;[7] this stems from the arbitrary alignment of the droplet directors in the quiescent state, where some droplets will require a higher voltage to fully reorient with the field than others. This is, however, fortuitous from the perspective of achieving *grey-scale*. *Hysteresis* is defined as the difference in voltages required to switch a PDLC to 50% *transmission*, *before* and *after* it has been fully switched ON; its existence in the electro-optical response, due to friction at the LC/polymer interface, may also cause problems for displays with a high information content.[7,8]

2.5.7 Switching Speeds

More precise expressions exist for the rise and decay times, where the rise time, τ_{on} (which is technically the time elapsed in going from the OFF state, 0%, to 90% of the ON state transmission), is given by:[8]

$$\tau_{on} = \frac{\gamma_1}{\varepsilon_0 \Delta\varepsilon E^2 + \frac{K\left(l^2 - 1\right)}{a^2}} \quad \textbf{(14)}$$

where γ_1 is the *rotational viscosity* of the LC (which will suffer an increase with the inclusion of dye dopants), ε_0 is the *permittivity of free space*, and E ($=V/d$) is the applied field. It can be seen from **(14)** that the more deformed a droplet is (i.e. the larger l is), the shorter the rise time is; also, larger droplets are allegedly conducive to longer rise times. It is difficult to make a comparison between this expression and equations for the rise time of conventional LCDs. Spherical droplets apparently yield no dependence of the rise time on droplet size, but this is a moot point. Exclusively in the case of spherical droplets, it can be seen that:

$$\tau_{on} \propto \frac{1}{E^2} \quad \textbf{(15)}$$

where the constant of proportionality is termed the *speed factor*. An expression for the decay time, τ_{off} (which is technically the time elapsed in going from 100% to 10% of the ON state transmission, upon removal of the field), is ascertained by putting E=0 in **(14)**, yielding:[5,8,15,16]

$$\tau_{off} = \frac{\gamma_1 a^2}{K\left(l^2 - 1\right)} \quad \textbf{(16)}$$

It can therefore be seen that τ_{off} has the same dependence on droplet size and shape as τ_{on}, but **(16)** does not apply to PDLCs with spherical droplets; decay times of PDLCs are typically much faster than those of conventional LCDs, especially for small, highly ellipsoidal droplets.[5] **(16)** only applies to a PDLC which has been fully switched ON, since smaller applied fields (i.e. less reorientation) will result in faster decay times. It is also apparent that there exists a trade-off between achieving a low switching voltage and low switching speeds, hinged upon the size and shape of the droplets. Methods of achieving ellipsoidal droplets may include curing films at higher temperatures (as previously mentioned), or pausing the polymerisation mid-cure (after the onset of phase separation), then resuming it; applying pressure to the films, or an electric or magnetic field parallel to the substrates, during curing may also cause the formation of ellipsoidal droplets, but in this instance with their semi-major axes in the plane of the film. Although this may lead to larger rise times due to considerably increased anchoring energy opposing director reorientation from the plane of the sample (albeit not apparent from **(14)**), and have a detrimental effect on the switching voltages, dye-doped films would be expected to be more coloured for such a morphology, due to the optimum alignment of the dye molecules' axes of maximum absorption.

3. EXPERIMENTAL MATERIALS, METHODS, RESULTS, AND DISCUSSION

3.1 Material Properties

3.1.1 BL001 Liquid Crystal Properties[22]

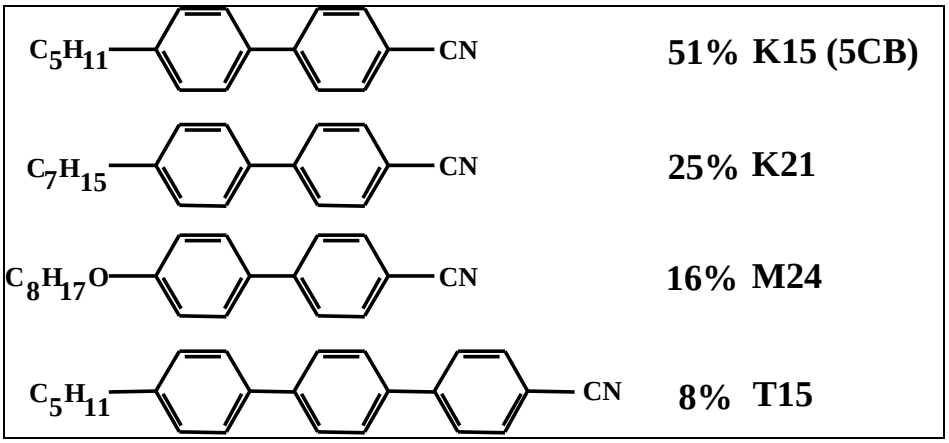

Fig.7: The chemical structure of the constituents of Merck's liquid crystal BL001 (formerly E7)

$n_o=1.5216$, $n_e=1.7462 \Rightarrow \Delta n=0.2246$ (all values at 589 nm, 20° C)

$\varepsilon_{\perp}=5.2$, $\varepsilon_{//}=19.0 \Rightarrow \Delta\varepsilon=13.8$ (all values at 1 kHz, 20° C)

N-I transition (clearing point) temperature=*61° C*; freezing point=*-10° C*; boiling point>*200° C*; density≈*1 g/ml*; resistivity=$4x10^{11}\ \Omega m$

3.1.2 NOA 65 Polymer Properties[23,24]

NOA (Norland Optical Adhesive) 65 is a clear, colourless, liquid photopolymer that cures in ultraviolet light (with a maximum absorption in the range of 350 to 380 nm). The cured adhesive is very flexible, and was designed to minimise strain. Before and after cure, its transmission has no spectral dependence across visible wavelengths. It consists of a *backbone polymer* (modified urethane acrylates), *photo-initiator* (benzophenone), and *linking polymer* (timethylolpropane diallyl ether, trimethylolpropane tris thiol, isophorone, di-isocyanate ester). It has the following properties:

Refractive index of cured polymer**,** $n_p=1.524$; curing temperature range: *-15* to *60° C*; dielectric constant of cured polymer, $\varepsilon_p=8\pm1$ (experimentally determined using *Hewlett Packard 4278A* capacitance meter, at 1 kHz, 20° C)

It can be seen that this refractive index is compatible with the ordinary refractive index of BL001 (only mismatched by *0.0024*, and it has been reported[25] that no appreciable scattering occurs when the mismatch≤*0.002*). From the perspective of **(1)**, the refractive index mismatch in the OFF state has a mean value of *0.11* (*0.10* from **(2)**), which should be conducive to significant scattering. The wavelength dependence of the refractive indices of the polymer and LC is expected to be negligible. It is found that the solubility maximum of BL001 in NOA 65 at room

temperature is *66.4 w/w %*.[8] The dielectric constant of the polymer is larger than the perpendicular dielectric constant of the LC, which is ideal from the perspective of **(12)**, which predicts that the ratio between the E-fields in the LC and the polymer is *~110%* in the ON state and *~85%* immediately after application of the field, where *150%* is optimum.

3.1.3 Dichroic Dye Properties

A suite of dichroic dyes consisting of 17 *IRL (Industrial Research Limited) New Zealand dyes* and 4 *Niopik Russian dyes*, of a variety of colours, are to be investigated in this work. The IRL dyes are thought to be highly dipolar (being *merocyanine* dyes), in contrast to the low dipole moments expected in the Niopik dyes (being *dispersed azodyes*). Only 1 of the IRL dyes, *AK-00-41*, was found to be soluble in BL001, but all 4 Niopik dyes, *KD-8*, *KD-9*, *KD-10*, and *KD-184* were found to be readily soluble; the 16 dyes which were found to be insoluble are listed in **Appendix A**. **Fig.8** shows the chemical structure of AK-00-41, courtesy of IRL; chemical structures of the Russian dyes are not available from Niopik, but *nuclear magnetic resonance* (NMR) analysis reveals that the chemical structure of KD-184 is as depicted in **Fig.9**.

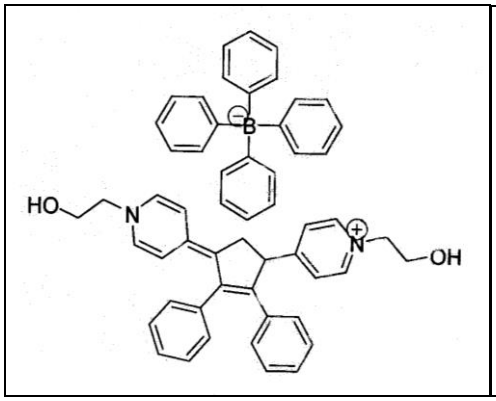

Fig.8: Chemical Structure of AK-00-41

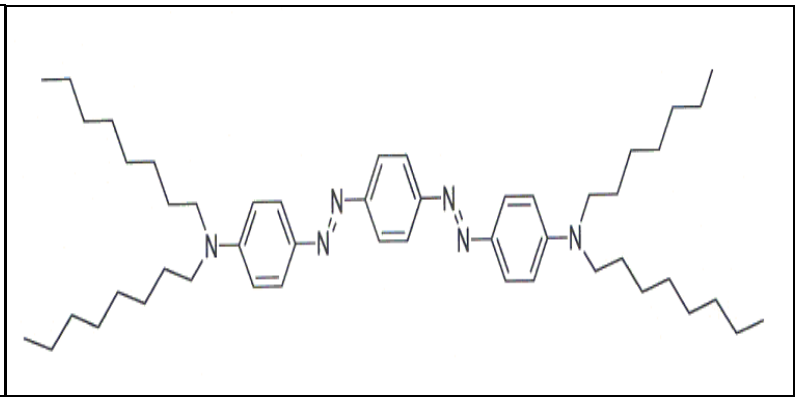

Fig.9: Chemical Structure of KD-184

Values for the *molecular weights* (MWs, also known as *molar masses*) of dyes are not available from IRL, but chemical structure analysis has been used to ascertain the value for AK-00-41, given in **Table 1**, which also contains the MWs of the Russian dyes, supplied by Niopik. Values of the order parameters measured[26] for the soluble dyes in BL001 (at approximately 1 w/w % dye concentration) are also quoted in **Table 1**.

Dye	Colour in BL001 LC	Molecular Weight/Molar Mass [g]	Order Parameter, *S*
AK-00-41	Orange	783	0.1
KD-8	Light Yellow	910	0.7
KD-9	Yellow	486	0.7
KD-10	Blue	532	0.8
KD-184	Red	765	0.7

Table 1: Important dye parameters for the dyes which were found to be soluble in BL001 LC

The Niopik dyes clearly align much better with the LC molecules than the IRL one, due to their considerably higher order parameters, and this may be explained by observation of **Figs.8** and **9**, which show how the IRL dye

possesses no obvious long molecular axis, whereas one of the Niopik dyes does. The values of order parameter are expected to have only a slight dependence on dye concentration.

For these dyes to be suitable for inclusion in PDLCs, it is important that they exhibit low absorption of light at the wavelength of curing (i.e. 365 nm for UV curing), otherwise the dye may suffer photodegradation during the curing process, impairing its colour; the rate of polymerisation will also then heavily depend on the dye concentration, complicating the curing procedure. It is therefore useful to ascertain *absorption spectra* of the dyes, in a variety of solvents, and this was achieved using a *Perkin Elmer UV/VIS/NIR Lambda 19 Absorption Spectrometer*. Solutions containing a small quantity (~1 mg) of each dye dissolved separately in *Methanol* (MeOH) and *Acetonitrile* (ACN) were prepared, and individually placed in the "first arm" of the spectrometer, in a quartz cuvette, with a cuvette containing only the relevant solvent placed in the "second arm" of the spectrometer, to correct for the absorption due to the solvent. The spectrometer then shines light of a range of wavelengths through both cuvettes, measuring the absorption of each, subtracting that in the second arm from that in the first arm. KD-8 was found to be insoluble in both MeOH and ACN, so its spectrum was measured by using *Dichloromethane* as a solvent. The spectrometer is able to measure values of absorption up to *6 OD*, but any value above *4 OD* is deemed untrustworthy, hence some solutions required dilution with the relevant solvent, to reduce the dye absorption. The compiled data was then normalised so that the largest peak of absorption in the visible range of wavelengths had a value of *1*; this data is shown in **Graph 1**, where the spectra are colour-coded to the colour of the dyes.

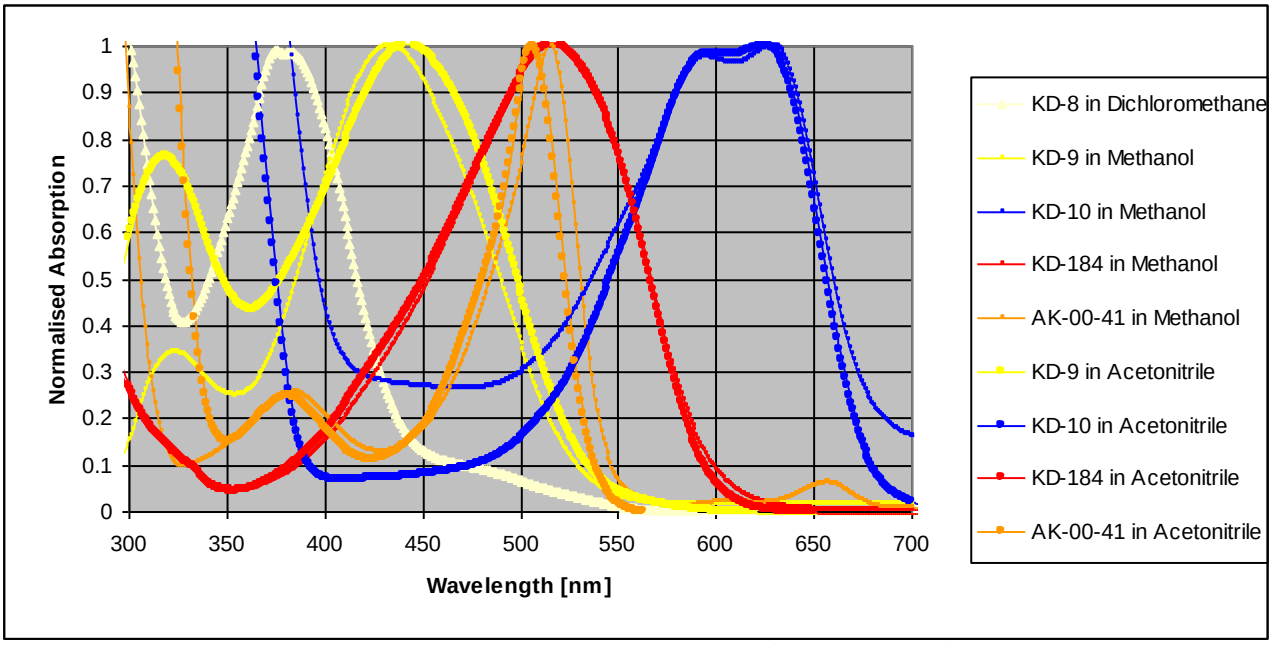

Graph 1: Colour-coded, normalised absorption spectra of dyes, in a variety of solvents

It can be seen from **Graph 1** that KD-8 and KD-10 both have a very high absorption at UV wavelengths (365 nm), probably rendering them unsuitable for PDLCs made with UV curing. KD-9 and AK-00-41 both seem adequate, but KD-184 can be seen to be very suitable for UV curing. However, all the dyes except KD-8 and KD-9 have low absorption at 400 nm, which is the wavelength at which the visible-curable monomers, *NOA 72* and *NOA 76* (in

conjunction with the Merck LC, *BL024*), are cured. Hence, an attempt was made to create PDLCs with all 5 dyes using visible curing, but it was found that achieving uniform polymerization across the LC cell was extremely difficult, due to the availability of only a low intensity 400 nm source. It was found that the IRL dyes AK-00-35, AK-00-37, AK-00-38, and AK-00-41, also exhibited very low absorption at 400 nm, but they were found to be insoluble in BL024, just as they were insoluble in BL001; it was deemed futile to continue research with visible curing, but this may be a fruitful area for future research if a high intensity, 400 nm source could be acquired, especially for KD-10. The fact that the peaks of absorption for each dye are at approximately the same wavelengths for two different solvents suggests that the spectra for the dyes in LC will be very similar.

It is useful to know values for the extinction coefficients of the dyes, since this information can be used to gain insight into the dye concentration in a PDLC cell. From **(8)**, it can be seen that the extinction coefficient of a dye [molar^{-1} cm^{-1}] is the gradient of a graph of absorption [OD] versus concentration [molar]. Thus, each of the dye solutions in ACN, of known dye concentration, was half diluted with ACN several times, and the absorption spectrum was taken for each concentration, to yield a value for the maximum absorption. The use of MeOH as a solvent would be expected to yield the same results as with ACN. **Graphs 2(a)** to **(d)** show this information, for all the dyes except KD-8 – dichloromethane is carcinogenic, hence it was deemed too hazardous to perform the experiment.

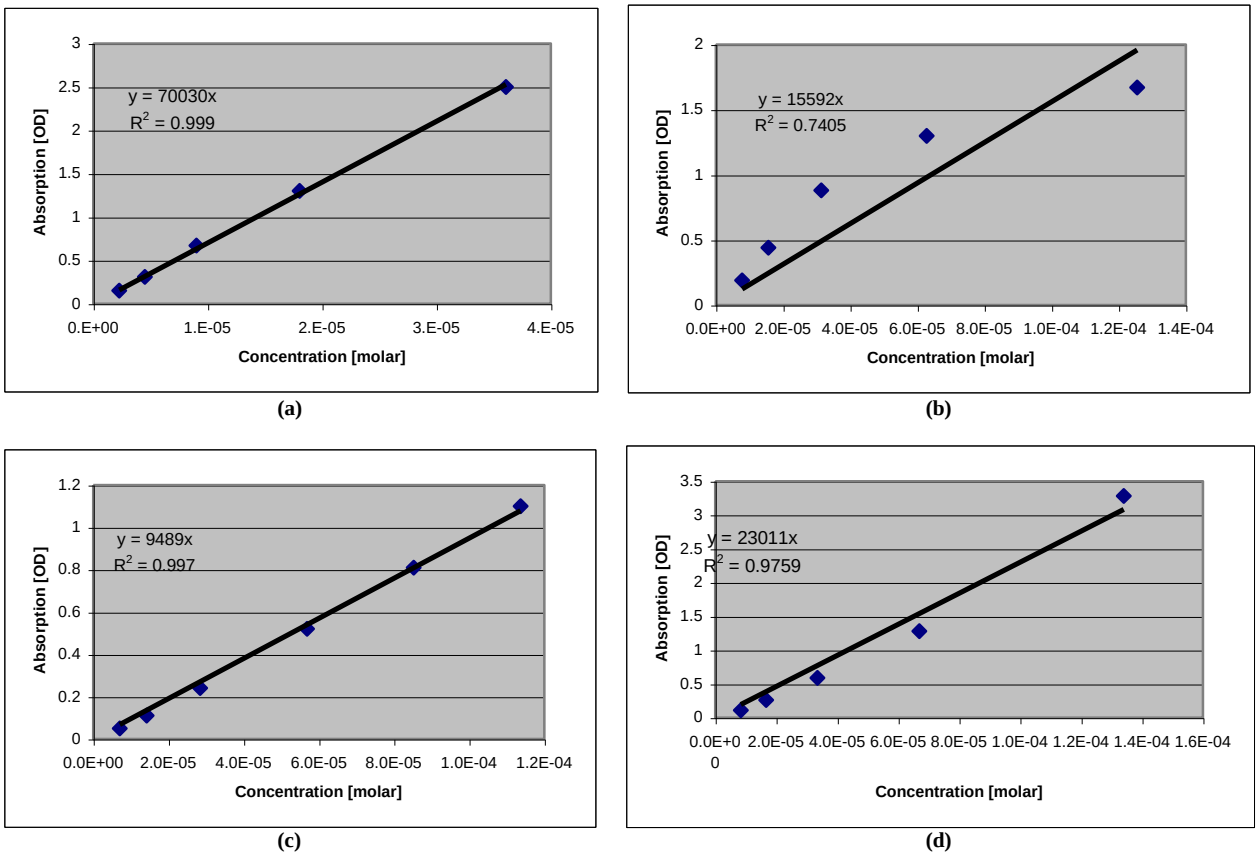

Graph 2: Dependence of dye absorption upon dye concentration for **(a)** AK-00-41, **(b)** KD-9, **(c)** KD-10, and **(d)** KD-184

Dye	Extinction Coefficient [per molar per cm]	R^2
AK-00-41	70030	0.999
KD-9	15592	0.741
KD-10	9489	0.997
KD-184	23011	0.976

Table 2: Values for the extinction coefficients of the dyes, and a measure of their accuracy

The lines of best fit in **Graphs 2(a)** to **(d)** have been forced to intercept the origin, to comply with the definition of absorption in **(8)**. **Table 2** gives a summary of the data from the graphs, where it can be seen that the values of extinction coefficient are given to high accuracy, except in the case of KD-9, which would not fully dissolve in the ACN, even with extended heating and stirring. It is also apparent from **Table 2** that the IRL dye consists of molecules that absorb considerably more light than the Niopik dyes' molecules.

3.2 Fabrication of an Undoped PDLC

The great difficulty in making a PDLC mixture is in accurately measuring the small quantities of LC and monomer involved (since LC is a very expensive material). 100 μl is typically the quantity of each used for each mixture, but it ideal to express LC concentration in the monomer by w/w %. The commonly used approximation is that LC and monomer both have the density of water, so that 100 μl=100 mg, but this is not a good assumption. Measuring such small quantities requires the use of a micropipette (*Volac High Precision Micropipette*, not calibrated below 100 μl), where measurements of the masses of 3 samples of "100 μl" of pure water gave a mean mass of (96.2±0.3) mg (measured on *Oertling NA114 Digital Scales*, accurate to the nearest 0.1 mg); "50 μl" of water was measured to be 49.7 mg, and "150 μl" was measured to be 146.9 mg. These anomalies may be attributed to the viscosity of water preventing all the water from exiting the pipette spout. BL001 and especially NOA 65 are more viscous than water, so that a measurement of volume of these materials with this micropipette is likely to be appreciably smaller than the desired volume. Measurements of the masses of 10 samples of "100 μl" of BL001 gave a mean mass of (109.1±0.6) mg; measurements of the masses of 10 samples of "100 μl" of NOA 65 gave a mean mass of (121.8±7.1) mg; measurements of the masses of 10 samples of "50 μl" of NOA 65 gave a mean mass of (65.3±5.4) mg. For measuring volumes of NOA 65, ~1 cm at the end of the pipette spout had to be cut off to facilitate the removal of the highly viscous monomer. When attempting to achieve a certain w/w % of LC in the monomer, these relations between volume and mass were utilized. If, for instance, a LC concentration of 67 w/w % was desired, this would be achieved by mixing "100 μl" LC with "42 μl" monomer.

All creation of mixtures had to be performed in the protective nitrogen atmosphere of a *glove-box*, since LC molecules react with moisture in the air. A small, plastic container (*Samco COC Vial*) with a lid was weighed, placed in the glovebox, then filled with the required volume of LC using the micropipette. The lid was able to hermetically seal the container, so it was then safe to remove the container from the glovebox, after which it was re-weighed and placed

back in the glove-box. The required volume of monomer was then added to the LC, using a fresh spout. After removal from the glove-box again, the container was weighed once more, then sealed with stretchable film around the cap, as a precautionary measure. The container was then placed in an *ultra-sound/sonic bath*, in which it was vibrated at very high frequency in water, and left for at least 2 hours, after which the water had heated up to above 50° C. It was *assumed* that this process was sufficient to homogeneously disperse the LC molecules throughout the monomer.

The glass LC cells (*E.H.C. Co., Ltd., PI=X, 2.5 by 2 cm*) were unaligned, and supposedly have a cell spacing of 10 μm. This was tested by using the capacitance meter to measure the capacitances of 10 cells, and the mean cell gap was found to be (9.84±0.2) μm (assuming that the1 cm^2 ITO had complete overlap of electrodes). It is thought that the electrodes are coated with a very thin protective layer of *unrubbed* polyimide, which will mean that the actual cell gap will be slightly smaller. After placing the cell and mixture in the glove-box, the cell was heated on a hotplate to about 70 or 80° C; this temperature could only be very roughly determined by using an infra-red thermometer (*Cole Parmer Digi-Sense DuaLog R*) to detect the thermal radiation emitted. A pipette spout was used to remove a small amount of the transparent mixture from the container, and then its tip was placed against one edge of the LC cell. The reduction of the viscosity of the mixture, due to the heating of the cell, led to the mixture filling the cell by virtue of the capillary action. Once filled with mixture, it was important to protect the cell from ambient light (which contains a vestige of UV radiation), lest unwanted curing of the monomer may result. Filling temperatures of up to 150° C were found to produce no detectable change in the finished morphology of undoped PDLCs; such temperatures mean that cells fill faster, but caution must be taken for temperatures approaching 200° C, BL001's boiling temperature. Filling cells at room temperature was found to lead to the presence of air bubbles in the film, as well as being very time-consuming. Once a cell was filled, it was safe to remove it from the glove-box, since now only LC at the edge was exposed to the air.

The cell was then ready to be cured under the UV lamp (*Spectroline EN-180L/F, 50 Hz, 230 V, 0.17 A* $\Rightarrow$ *P=39.1 W)*. The area of UV emission on the lamp was about 20 cm by 5 cm in area; since it is not from a point source, it would be extremely difficult to determine the intensity of light received at a point a certain distance away from the lamp, as the intensity is not related to distance by the usual inverse square law; the use of a photodetector was ruled out as it was often necessary to cure cells at very small distances (i.e. ~0 cm) from the lamp. Hence, the curing distance from the lamp is the only means viable to quantify the intensity of light incident on the PDLC.

The PDLC was placed below the center of the area of UV emission, on a white background (i.e. blank paper, to reflect UV light back through the PDLC), at a certain distance from the lamp. The largest curing distance used was 15 cm, and undoped PDLCs were found to be fully cured within a minute at this distance; however, to ensure full polymerization of the monomer at all heights of curing, all undoped PDLCs were individually cured for 2 minutes. Curing a fully-polymerised PDLC for a further 10 minutes at 0 cm from the lamp was not found to appreciably change

its electro-optical properties, so the fact that PDLCs cured close to the lamp will receive far more UV energy has negligible implications. The temperature at which a PDLC was made was always noted, but the error on this may be as much as 2 or 3° C. Maintaining a constant PDLC-temperature during the curing process was very important; achieving this condition below room temperature was impossible with the equipment available, and achieving this above room temperature was very difficult (since only hotplates were available, and they are not able to maintain a constant temperature for more than 1 minute). **Figs**.**9(a)**, **(b)**, **(c)**, **(d)**, and **(e)** show the appearance of a PDLC before and after the curing process; the ON state is achieved by applying a sine-wave voltage of 15 V_{rms} across the ITOs (which was found to be sufficient to fully switch this PDLC), accessed at the substrate edges, at 1 kHz, using a *signal generator* with a *step-up transformer*.

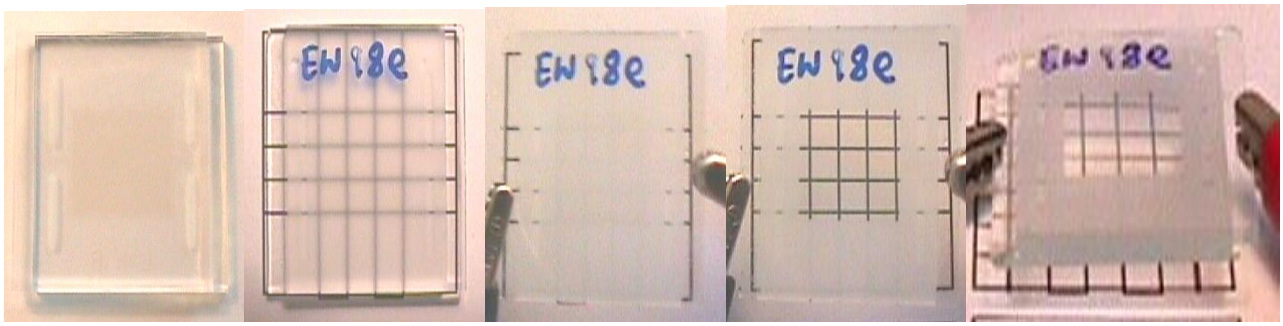

(a) **(b)** **(c)** **(d)** **(e)**

Fig.9: Photos of a PDLC cell, **(a)** before curing, which resembles an empty cell (note the ITO is visible), **(b)** after curing, against grid surface, in the OFF state, **(c)** 1 cm from grid surface, in the OFF state, demonstrating the high opacity, **(d)** 1 cm from grid surface, in the ON state, demonstrating the high transparency across the ITO region, and **(e)** 1 cm from grid surface, in the ON state, at a viewing angle of ~60°, demonstrating the high transparency of the ON state even at large viewing angles (note that the dark region in the upper half of the ITO region is caused by shadow). This particular PDLC has a LC concentration of 60 w/w %, and was cured at 7 cm from the UV lamp, at 22° C

Graph 3 shows how an empty LC cell is susceptible to *thin film effect interference*, due to constructive and destructive interference between light that is forward-propagating, and back-reflected from the glass substrates. This phenomenon is virtually eliminated once the cell is filled with media that has a similar refractive index to that of glass (i.e. 1.5), since reflection of light from an interface is a strong function of refractive index mismatch. Hence, filled cells are much more suitable for use in normalizing transmitted intensity data.

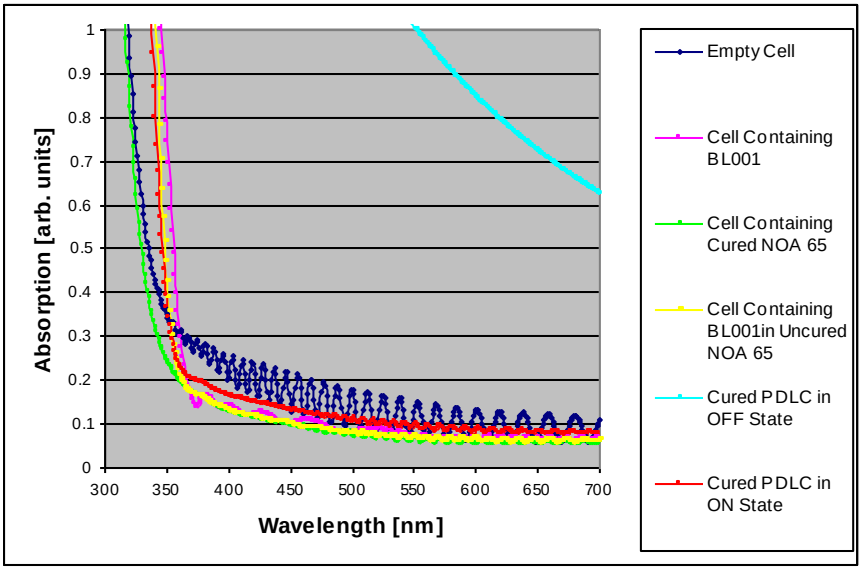

Graph 3: Absorption spectra showing how an empty LC cell is prone to *thin film effect interference*, but this is virtually eliminated for a filled cell. BL001 can be seen to absorb significantly at 350 nm, just below the UV cure wavelength. Cured and uncured (not shown) NOA 65 have almost identical spectra. It can be seen that NOA 65 has an almost identical spectrum to LC in uncured NOA 65, across visible wavelengths. The cured cell can be seen to have an ON state almost as transparent as an empty cell. The OFF state scattering can be seen to be inversely proportional to the wavelength to some power, as predicted. Using **(10)**, this cell has an optical density contrast ratio of approximately 10, at 633 nm

The cell containing BL001 in uncured NOA 65 (50 w/w %, but other LC concentrations produced virtually identical spectra) would be most suitable to normalize transmission data, if it were not for the fact that it may gradually cure in ambient light, possibly causing phase separation leading to scattered light; since the cell containing cured NOA 65 can be seen to have an almost identical spectrum over visible wavelengths, this cell was deemed to be the most suitable for normalization purposes, as it is chemically stable.

Fig.10 shows a typical undoped PDLC between crossed polarisers, under a 20x microscope (i.e. *polarized microscopy*), demonstrating the birefringence of the LC droplets. Applying a sufficiently large electric field to the PDLC causes all the birefringence to disappear, rendering the droplets invisible. Unfortunately, it is extremely difficult to deduce the average droplet size and shape from this image, and a more powerful microscope was not available. A very rough estimate is that the droplets are ~1 μm in diameter.

Fig.10: Photo of typical PDLC, taken using polarised microscopy

Mixtures containing 24, 35, 41, 48, 53, 60, 65, and 74 w/w % LC in monomer were prepared; it is very difficult to estimate the errors in these concentrations, since the largest source of error is likely to be due to the LC molecules not being homogeneously dispersed throughout the monomer. Indeed, it was found to be almost impossible to create uniformly-polymerised PDLCs using the first three concentrations, since the mixture was too viscous to allow homogeneity to be achieved via placement of the mixtures in the sonic bath. *Magnetic stirring bars* were placed in the mixtures, and the containers were left on a *stirrer* for several hours; this produced no improvement, so these mixtures were abandoned. The 74 w/w % sample suffered a similar problem, but this was due to the fact that the solubility maximum had been exceeded, so regardless of how long the mixture was stirred for, the excess LC would never become dissolved; this mixture was also discarded. The remaining 4 mixtures were used to fabricate PDLCs at curing distances varying from 0 cm to 15 cm, at a variety of curing temperatures varying from 22 to 41° C. Measuring the viewing angle dependence, CR, hysteresis, switching voltages, and switching speeds of these cells should allow insight to be gained into how and why these properties are determined by the morphology of the polymeric binder.

3.3 Experiment 1: Viewing Angle Dependence

3.3.1 Experimental Procedure

The first goal is to try to gain insight into the droplet size of a PDLC, as well as assess the angular extent of the scattered light. **Fig.11** shows the experimental set-up, where adjustable mirrors were used to finely direct the laser beam (λ=633 nm) to be normally incident on the photodetector when the rotating arm was at θ=0°, in the absence of a PDLC. Photomasks with circular apertures of ~1 mm were placed in front on the photodetector, to prevent it from receiving unwanted reflections of light, and also to facilitate the exact placement of the PDLC on the central, stationary platform. The linear response of the photodetector to light was tested by using *Malus' law*, and a plot of intensity (i.e. readings of the photodetector output voltage on the voltmeter) against the square of the sine of the angle between the transmission axes of 2 linear polarisers placed in the path of the beam, yielded a R^2 value of 0.99995. *Neutral density filters* were used to confirm that this linearity remained intact for light intensities up to the photodetector's *saturation point*.

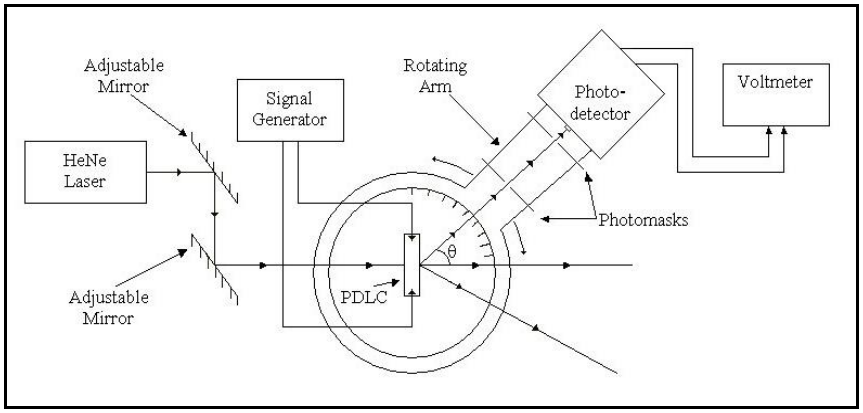

Fig.11: Scheme of the experimental set-up used in viewing angle dependence measurements

A PDLC was placed on the stationary platform, about which the arm rotates, to intercept the laser beam at normal incidence; to ensure that the beam was incident on the PDLC at the centre of rotation of the arm, the arm was rotated to wide angles and fine adjustments of the placement of the PDLC were made until the light passing through the first photomask was able to pass through the second unimpeded, and into the photodetector. The signal generator was attached to the PDLC, and set to apply a 1 kHz sine-wave voltage such that the PDLC could be switched fully ON.

The use of a *two-phase lock-in amplifier*, in tandem with a *chopper* placed in the path of the beam, was experimented with, as a means of measuring the photodetector's output to high sensitivity, but this method was found to be very time-consuming, and stable readings were difficult to obtain. The use of a voltmeter, instead, means that all measurements must be performed in complete darkness, to ensure that the photodiode's response is solely due to light scattered from the PDLC. Readings of photodetector voltage were taken for scattering angles from 0 to 15°, in 0.5° increments, from 15 to 20°, in 1° increments, and from 20 to 170°, in 5° increments, for PDLCs in the OFF state; for the ON state, angles from 0 to 15°, in 1° increments, and from 15 to 170°, in 5° increments, were used. These measurements were performed on PDLCs with 48 w/w % LC, cured at distances of 0, 1, 3, 5, 7, 9, 11, and 15 cm (at 22° C), as well as on PDLCs with 65 w/w % LC, cured at distances of 0, 1, 3, 5, 7, 9, and 15 cm.

3.3.2 Results and Discussion

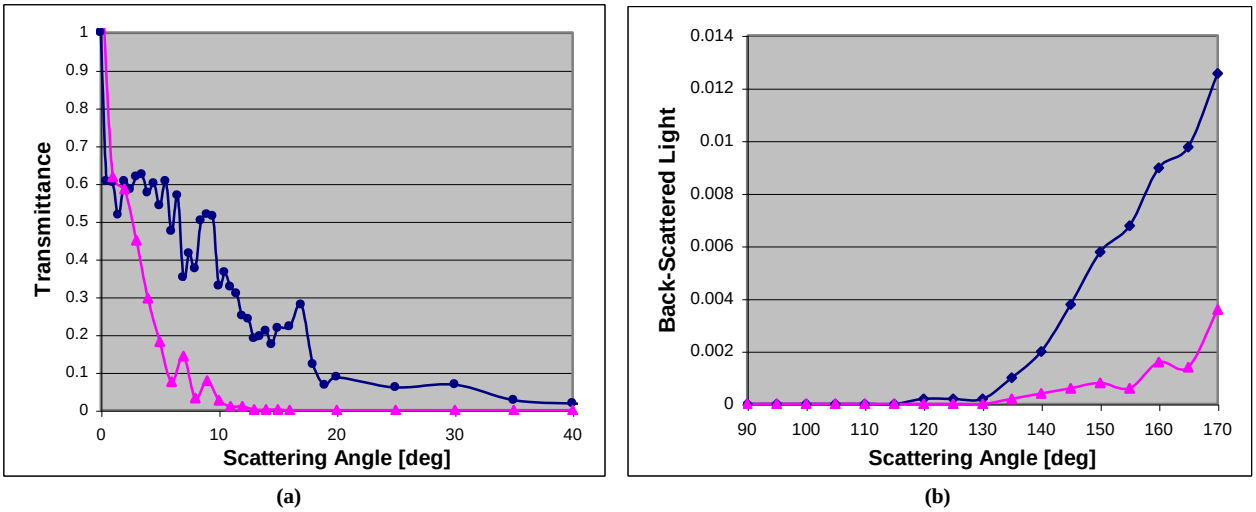

(a) **(b)**

Graph 4: The angular dependence of light scattered from a PDLC with 48 w/w % LC, cured at 3 cm, at 22° C, for **(a)** forward-scattered light, and for **(b)** back-scattered light, where the circles represent the OFF state, and the triangles represent the ON state

Graphs 4(a) and **(b)** show the viewing angle dependence for a PDLC with 48 w/w % LC, cured at 3 cm, at 22° C; however, this data typifies the results found for *all* the PDLCs tested. The widths of the central maxima were found to vary from about 10 to 20°, but no trend could be deduced; hence, the relative droplet sizes cannot be ascertained from this method. For *all* the PDLCs tested, a vestige of scattered light could be detected out to 80 or 85°. In the PDLC ON state, the photodiode was found to be saturated, but it was deemed inappropriate to use neutral density filters to attenuate the intensity, since this would lead to decreased sensitivity of the apparatus. Thus, instead of normalising the data with respect to the transmission of a cell filled with cured NOA 65, at 0°, it was normalised to the transmission of the OFF state (for both **(a)** and **(b)**). It can be seen from **(a)** that the intensity distribution is very complicated, suggesting a distribution of droplet sizes; indeed, repeat measurements on some PDLCs, with the laser beam impinging on a different part of the PDLC, revealed a noticeably different intensity profile. From **(b)**, the back-scattered light can be seen to be only a tiny fraction of the transmitted light; for $\theta>170°$, the photodetector obscured the laser beam.

A Guinier plot was made for all the PDLCs tested, but the results are inconclusive. If we anticipate that the droplets are ~1 μm in diameter, then **(3)** is only valid for angles of scattering, $\theta=6°$, but the Guinier plots revealed no linearity for such small angles. Interestingly, however, plots for 4 of the PDLCs *were* linear out to angles as large as 15°, having R^2 values of close to 0.9. **Graph 5** shows the Guinier plot for the PDLC whose data is shown in **Graphs 4(a)** and **(b);** using its gradient, and **(3)**, the mean droplet diameter is estimated to be 0.8 μm, but this is outside of the range of validity of the Guinier plot. The other plots predicted similar droplet sizes, but there existed no trend between them. Repeat measurements either yielded Guinier plots that predicted appreciably different droplet sizes for the same PDLCs, or plots that had no linearity. Hence, it appears that the Guinier plot is *not* suitable for estimating the droplet sizes of PDLCs, except perhaps in the case where the scattering angles can be measured to tiny fractions of a degree.

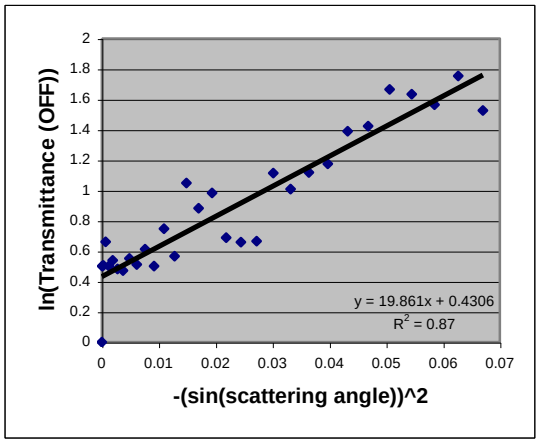

Graph 5: Guinier plot for data given in **Graph 4(a)**

3.4 Experiment 2: Contrast Ratio

3.4.1 Experimental Procedure

Since there will be an optimum droplet size for scattering, measurements of the contrast ratios of PDLCs made with different LC concentrations, curing distances, and curing temperatures, may elucidate how these different preparation conditions affect the droplet size. **(10)** shows how the OD CR is obtained from measurements of the absorption of a PDLC in the absorption spectrometer. Unfortunately, the narrow beam in the spectrometer is the same size as the ITO cell, thus placement inside the device was absolutely critical; hence, extra special care was taken to ensure that all PDLCs were placed in the same position for each measurement, and were immaculately cleaned. The second arm of the spectrometer was left vacant, because correction for the presence of the glass can be performed later.

(11) can be used to calculate the CR from measurements of the transmitted intensities, and the experimental set-up used to measure these values is depicted in **Fig.12**. Here, a circular aperture of ~35 μm is used to create a diffraction pattern of Airy discs from the laser beam, and from Rayleigh's Resolution Criterion, it can be deduced that the central disc will have a diameter of ~1 cm at a distance of 20 cm from the aperture. Thus, placement of a converging lens, of focal length of 20 cm, 20 cm from the aperture, will result in a collimated laser beam of width 1 cm emerging the lens; this is absolutely ideal for illuminating the ITO of a PDLC. Obscuring the ITO, so that only secondary Airy discs were transmitted from the PDLC, was found to lead to a negligible voltage from the photodetector, in a darkened laboratory.

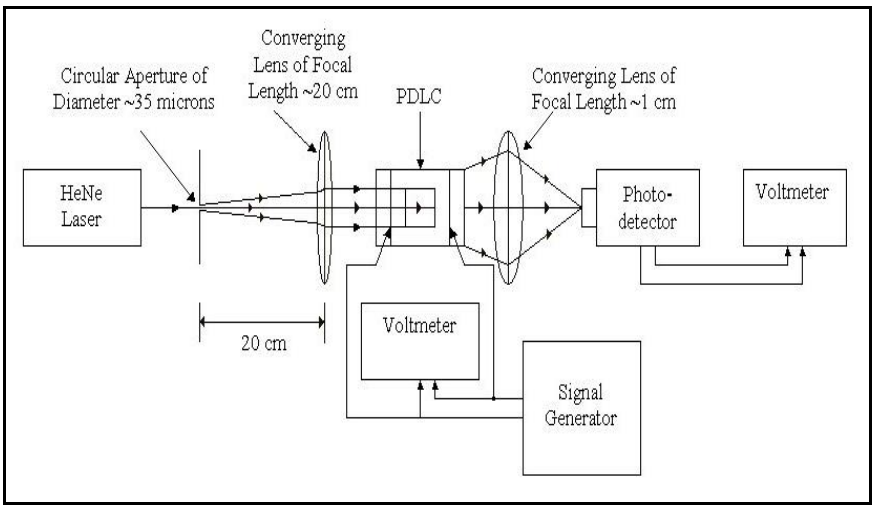

Fig.12: Scheme of the experimental set-up used for measurements of the contrast ratio of a PDLC, as governed by **(11)**

The distance between the PDLC and photodetector is critical in determining the magnitude of the measured CRs. It is futile to place the photodetector too close to the PDLC, because then the difference in measured transmittance between the ON and OFF states will originate solely from the reflection of light from the PDLC, which is very small, from the perspective of **Graph 4(b)**. Placing the photodetector too far from the PDLC will result in values of CR that are very sensitive to its scattering ability, but also to the placements of the PDLC and the second lens to intercept the beam, leading to irreproducible results. It was deemed appropriate to place the second lens (of diameter, 1.8 cm, and very small focal length) in the apparatus at a distance of 7 cm from the PDLC (which was the smallest possible distance due to constraints imposed by the lens holder), which will collect light scattered out to an angle of ~7°, and focus all of it into the photodetector. This distance should be conducive to CRs that accurately reflect the ability of a PDLC to scatter light, whilst maintaining a high degree of reproducibility. The PDLCs were fully switched ON, as before, with a sine-wave of frequency 1 kHz, so that the transmitted intensities in the ON and OFF states could be measured; the voltmeter placed in parallel was not necessary for this experiment. All measurements, once again, had to be taken under completely darkened laboratory conditions. The transmitted intensity of a cell containing cured NOA 65 was measured, so that the transmitted intensity of a PDLC could be normalised, even though this normalisation factor is cancelled out in the calculation of CR. Neutral density filters were used to remedy photodiode saturation.

3.4.2 Results and Discussion

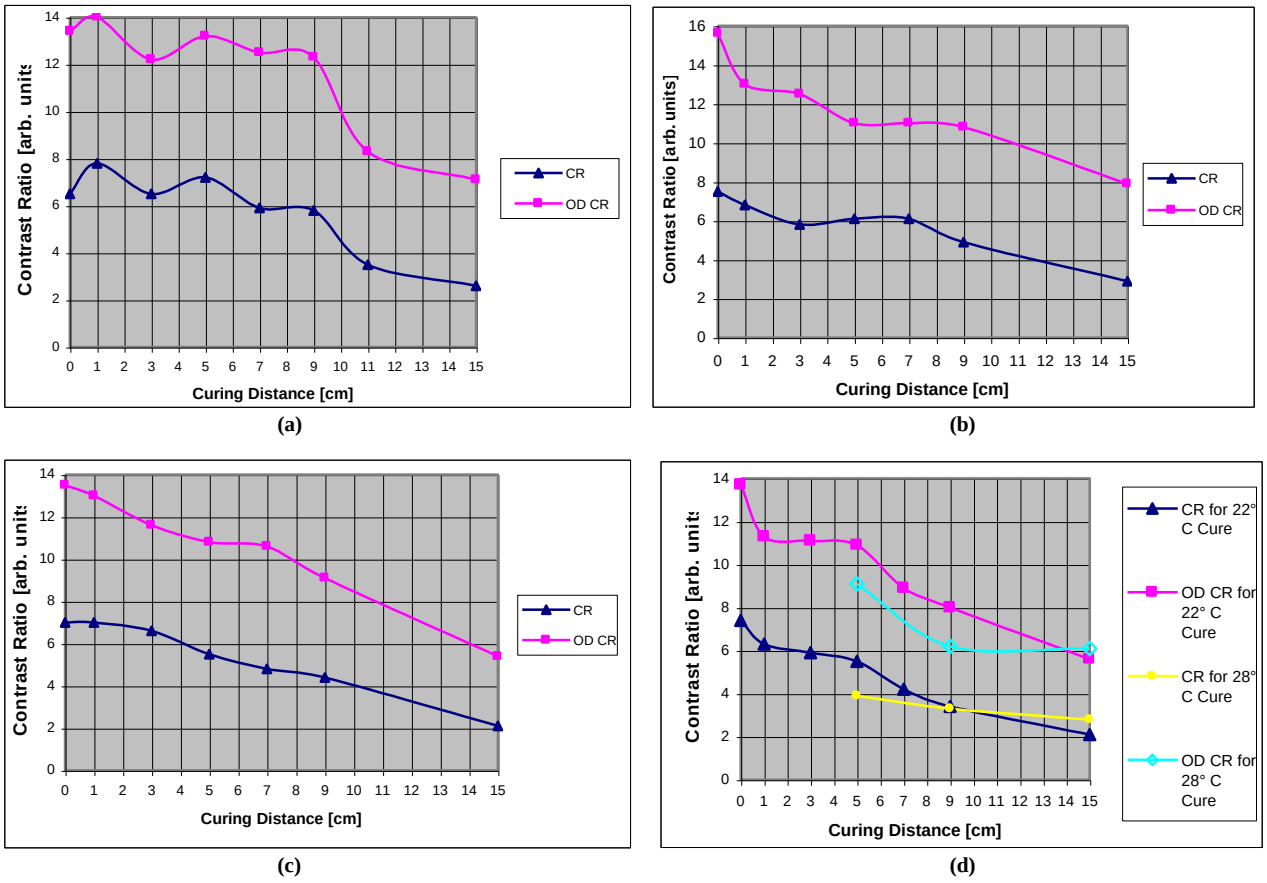

Graph 6: Values of CR and OD CR (at a wavelength of 633 nm) for a range of cure distances, cured at 22° C, for **(a)** 48 w/w % LC, **(b)** 53 w/w % LC, **(c)** 60 w/w % LC, and **(d)** 65 w/w % LC (which includes curing at 28° C)

Graphs 6(a) to **6(d)** clearly illustrate that a smaller curing distance is generally conducive to a higher contrast ratio, and there exists a strong relationship between values of CR and OD CR. The trend in **Graph 6(a)** may be explained by considering the fact that there exists an optimum droplet size for individual droplet scattering, but smaller droplets may create more scattering in a film simply because there is a greater number density of droplets. Thus, for 48 w/w % LC, the optimum droplet size seems to be obtained for curing at 5 cm, so curing closer to the lamp leads to smaller droplets which impair the scattering, until a point is reached (at a curing distance of 1 cm) where the number density of droplets is such that improved scattering is witnessed. The drop in CR and OD CR at 0 cm curing may be due to the rapid rate of polymerization leading to a significant quantity of LC molecules becoming permanently trapped in the polymer, leading to a reduced index mismatch. Another explanation for the peaks and troughs observed in **Graph 6(a)** is that mixtures with lower LC concentrations are more likely to contain inhomogeneities, hence each PDLC made with 48 w/w % LC mixture may have appreciable differences in LC concentration. Yet another justification is the fact that the values of CR and OD CR could have errors as large as ±1, due to the fact that the quantity is so sensitive to the placement of the PDLC in the path of the probing beam. It is useful to notice how the values of CR and OD CR arise from the values of transmittance and absorption; this data is shown in **Table 3**, for 48 w/w % LC.

Cure Distance [cm]	A(Off) [arb. units]	A(On) [arb. units]	OD CR	Corrected OD CR	T(On) [%]	T(Off) [%]	CR
0	0.87	0.065	13.4	55	0.99	0.153	6.5
1	0.97	0.068	14.3	51	0.95	0.123	7.8
3	0.88	0.072	12.2	38	0.88	0.135	6.5
5	1.03	0.078	13.2	35	0.86	0.12	7.2
7	0.99	0.079	12.5	31	0.82	0.14	5.9
9	0.95	0.074	12.8	38	0.83	0.143	5.8
11	0.74	0.089	8.3	18	0.81	0.23	3.5
15	0.63	0.089	7.1	15	0.8	0.307	2.6

Table 3: Values of absorption and transmittance, from which the OD CR and CR are derived, for 48 w/w % LC

It is apparent that the OD CR very closely follows the trend for the OFF-state absorption. It is also striking that the ON-state absorption generally increases for increased distances of curing – it would be expected that larger droplets would be conducive to less ON-state scattering due to the resulting lower number density of droplets. An explanation might be that larger curing distances are also likely to allow significant droplet deformation, which may prevent the complete reorientation of the droplet directors upon application of a field. Another reason for more deformed droplets is that larger droplets have a smaller surface area-to-volume ratio, resulting in less surface tension, meaning that larger droplets are far less likely to be perfect spheres than smaller droplets. Correcting for the presence of the glass substrates, by subtracting the absorption of a cell containing LC in uncured monomer (which is 0.05 arb. units, at 633 nm), results in very large values of OD CR that are very sensitive to the ON state absorption; a different trend is now observed for the corrected OD CRs. Due to this high dependence on a quantity that is so sensitive to placement of the PDLC in the spectrometer, the correction for the glass substrates is deemed unnecessary and inappropriate. The values

of transmittance also show that smaller droplets lead to a more transparent ON state, as well as the fact that it is the OFF-state transmittance which governs the CR; other LC concentrations generally show the same trends.

The higher LC concentrations, in **Graphs 6(b)** to (**d)**, appear to reach the optimum droplet size for scattering for curing distances closer to the lamp (which gives credence to the idea that larger LC concentrations are conducive to larger droplets), to coincide with the curing distance for optimized droplet number density. The fact that 0 cm curing leads to the best values of CR for these higher LC concentrations may suggest that *less* LC becomes permanently dissolved in the polymer, contradicting some reports,[8] or it may be that the effect of extra LC becoming permanently dissolved in the polymer, for high LC concentrations, is cancelled out by the optimum droplet size and optimum number density coinciding for small distances of curing. It is also apparent that higher LC concentrations only lead to higher contrast ratios for small distances of curing, since larger distances allow large droplets to form more quickly than they do for low LC concentrations.

Graph 6(d) shows that higher temperatures of curing lead to an improved contrast ratio only for large curing distances. This can be explained by considering that higher curing temperatures have two effects – the precipitation of smaller droplets, and more LC becoming permanently dissolved in the monomer (due to thermal oscillations of the LC molecules impeding the nucleation process, leading to a larger proportion of LC molecules remaining isolated in the polymer). For large curing distances, the effect of making the droplets smaller (thus taking them towards the optimum droplet size) has more impact than the decreased refractive index mismatch; the reverse situation is true for smaller curing distances. At a curing distance of 9 cm, it can be seen that a higher curing temperature has no effect on the CR, yet it has an appreciable effect on the OD CR; an explanation may be that curing at higher temperatures leads to a non-uniform morphology, and the CR and OD CR are measured using different beam sizes, hence different areas of the ITO are probed.

Graph 7 shows very high temperatures of curing are conducive to extremely low contrast ratios, due to very low OFF-state scattering as a result of considerable LC remaining dissolved in the polymer, and minute droplets. **Graph 7** also provides further proof that a slightly higher temperature of curing can lead to a higher contrast ratio, but only for large curing distances – in this case, 9 cm, for a 48 w/w % LC concentration.

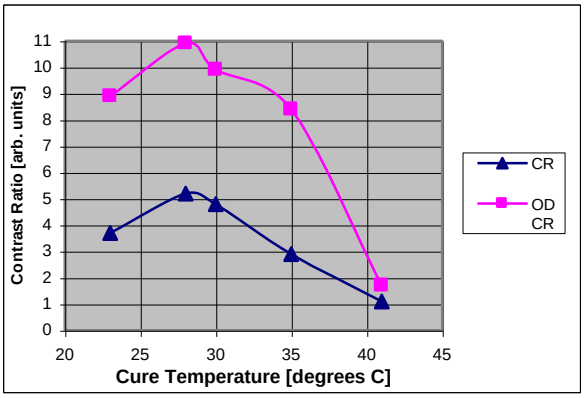

Graph 7: The dependence of contrast ratio on the curing temperature, for a LC concentration of 48 w/w %, cured at 9 cm

3.5 Experiment 3: Hysteresis

3.5.1 Experimental Procedure

The presence of hysteresis in the electro-optical characteristic may be problematic if PDLCs are to be used for displays involving moving images, thus it will be useful to identify its cause so that it can be eliminated. To do this, the experimental set-up from the previous experiment, depicted in **Fig.12**, was used. Decreasing the distance from the photodetector would mean that only hysteresis stemming from a change in the reflection characteristics of a PDLC could be detected, which would be almost immeasurable, from the perspective of **Graph 4(b)**; since a large degree of sensitivity is required in monitoring the relationship between the voltage applied to the PDLC and the photodiode voltage, it was deemed necessary to increase the distance from the PDLC to the photodetector to 40 cm (which was the largest distance allowed due to constraints imposed by the size of the optical bench).

Hysteresis is a time–dependent quantity, so the time elapsed between measuring the voltages to switch the PDLC to 50% transmission, before and after the cell has been fully switched on, has a large bearing on the measured values. It was deemed appropriate to measure hysteresis for both long and short durations between measurements, the latter being the most relevant. To observe the hysteresis for long durations between measurements, the electro-optical response curves of cells with 48 w/w % LC, cured at 3 and 11 cm, and a cell with 65 w/w % LC, cured at 9 cm, were measured.

This was achieved by slowly increasing the voltage applied to the PDLC (which had been vigorously tapped, since this is thought to facilitate director relaxation, and switched OFF for several days, to ensure that the cell harboured no hysteresis from previous experiments) from the signal generator, periodically noting the voltage from the photodetector with the corresponding applied voltage (from the voltmeter in parallel with the signal generator). At the point where a significant increase in the voltage provided no further increase in the transmitted intensity, the applied voltage was slowly reduced, again periodically noting how the photodetector voltage related to the applied voltage. At the point where the PDLC was fully switched OFF, the experiment was terminated. To convert the photodetector voltage into values of transmittance, the cell containing cured NOA 65 was used to ascertain the transmitted intensity from an “empty cell”. A plot of the electro-optical response can then be used to ascertain the hysteresis by calculating the difference in the applied voltages at 50% transmission. The experiment was timed so that approximately 1 minute had elapsed in reaching 50% transmission after the fully ON state. The hysteresis would be expected to have decreased somewhat from its maximum value, over such a long duration.

To calculate the hysteresis shortly after its formation, cells of 48 w/w % LC, cured at 0, 1, 3, 5, 7, 9, 11, and 15 cm, as well as 65 w/w % LC, cured at 0, 1, 3, 5, 7, 9, and 15 cm, were tested by measuring the photodetector voltages corresponding to 100% and 0% transmission (i.e. when the PDLC is on the ON and OFF states, respectively); the photodetector voltage corresponding to 50% transmission is simply the average of these two voltages. Again, these measurements had to be made on PDLCs which had not been switched fully ON for several days, and since the cells

had just been switched ON in ascertaining the voltage corresponding to 50% transmission, the PDLCs had to left for several more days before the experiment could be resumed.

The voltage applied to the PDLC was slowly increased until the 50% transmission voltage was attained on the photodetector, and this applied voltage was noted. The PDLC could then be fully switched ON by applying a very large voltage (i.e. ~90 V_{rms}) for a few seconds, then the applied voltage was carefully decreased to achieve 50% transmission again, and the required applied voltage was noted once more. The experiment was timed so that approximately 10 s had elapsed in achieving the 50% transmission state from the fully ON state. The hysteresis would not be expected to have decreased much from its maximum value, over such a short duration.

3.5.2 Results and Discussion

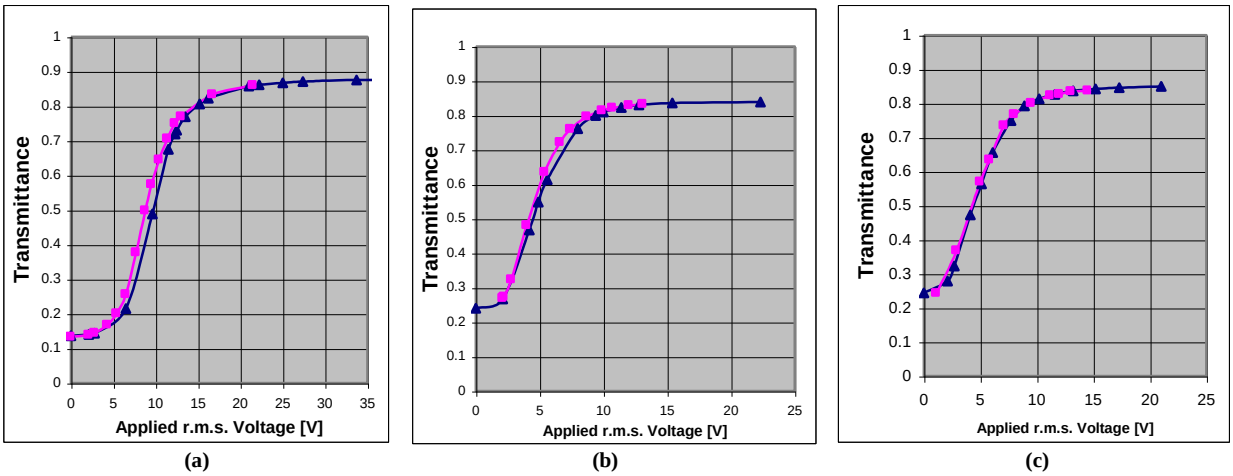

Graph 8: Electro-optical response curves/hysteresis loops for PDLCs cured at 22° C with, **(a)** 48 w/w % LC, cured at 3 cm, **(b)** 48 w/w % LC, cured at 11 cm, and **(c)** 65 w/w % LC, cured at 9 cm. The triangles represent increasing voltage, and the squares denote decreasing voltage. It is estimated that 1 minute elapsed in attaining 50% transmission after the PDLC had been fully switched ON

It can be seen from **Graphs 8(a)** to **(c)** that increasing the curing distance from 3 to 9 cm, for 48 w/w % LC, decreases the hysteresis from 0.90 V to 0.33 V, and using a larger LC concentration of 65 w/w % cured at 9 cm reduces the hysteresis still further, to less than 0.10 V. **Graph 9** shows the hysteresis data for the same LC concentrations, but for a wide range of curing distances, where the time elapsed in attaining 50% transmission from the fully ON state has been decreased from ~1 minutes to ~10 s.

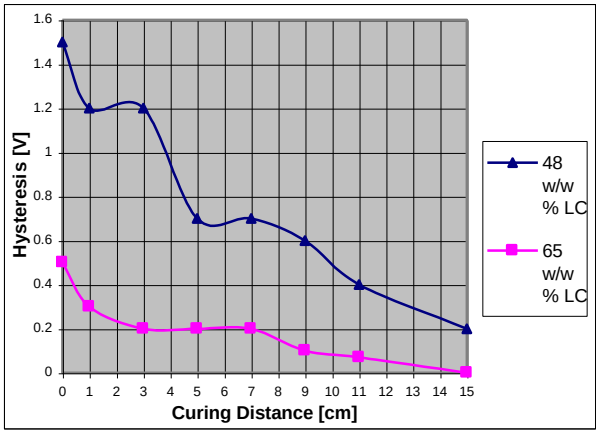

Graph 9: Hysteresis measured for PDLCs cured at 22° C, where it is estimated that 10 s elapsed in achieving the 50% transmission state from the fully ON state

It is readily observed from **Graph 9** that the hysteresis decreases significantly for larger distances of curing, and also by increasing the LC concentration. It can also be seen that the hysteresis from the PDLCs in **Graphs 8(a)** to **(c)** is now larger (0.90 V has now become 1.2 V, 0.33 V has become 0.4 V, and less than 0.1 V has increased to 0.1 V), due to less time being available for the hysteresis to decay. Error bars have been omitted from the graphs, in the interests of clarity, but due to the speed required in measuring the values, each value of hysteresis may have an error of ±0.2 V.

A simple explanation for the existence of hysteresis is that it originates from friction experienced by the LC molecules at the LC/polymer interface, so that after reorienting with an applied field, the droplet directors do not fully relax back to their original orientations immediately, as a result of LC molecules at the surface of the droplet being unable to slide back to resume their original positions and orientations. The effect that this has on the LC molecules in the interior of the droplet is largely determined by its size, where larger droplets are less influenced by the LC molecules at the surface of the droplet (i.e. they have a smaller surface-area-to-volume ratio), hence the droplet directors for such droplets are much more readily able to relax back. All droplet directors, regardless of droplet size, will eventually resume their original orientations, due to thermal oscillations of the LC molecules gradually aiding the movement of LC molecules at the droplet surface. It was observed that gentle tapping of a PDLC at 50 % transmission, after being fully switched ON, was sufficient to eliminate a substantial proportion of the hysteresis.

Hence, these results provide further proof that larger distances of curing, and larger LC concentrations, are conducive to larger droplets.

3.6 Experiment 4: Switching Voltages

3.6.1 Experimental Procedure

If PDLCs are to be used for portable displays (e.g. in mobile phones), it is a prerequisite that they require low voltages to switch. Using **(13)**, such measurements may also be used as a probe of droplet size and shape. To perform the measurements, the experimental set-up from the previous experiment, depicted in **Fig.12**, was used, where the distance of 40 cm from the PDLC to the photodetector was retained; leaving the distance at 7 cm would result in anomalously small readings of V_{10} and V_{90}.

Values of the photodetector voltage corresponding to maximum and minimum transmission of the PDLC (with the PDLC in the ON and OFF states, respectively) were measured for the non-dye-doped PDLCs that had not already been tested in the hysteresis experiment; again, these PDLCs were left for several days before subsequent experimentation. Values of the photodetector voltage corresponding to 10 and 90% transmission of a PDLC could then be calculated, by subtracting the 0% transmission voltage from the 100% value, multiplying this by 0.1 or 0.9, respectively, then adding the OFF-state (i.e. 0%) photodetector voltage. The applied voltage across the PDLC (again, a 1 kHz sine-wave) was then slowly increased until the photodetector voltage matched the 10% and 90% transmission voltages, and the required applied voltage (i.e. V_{10} and V_{90}) was noted in each case.

3.6.2 Results and Discussion

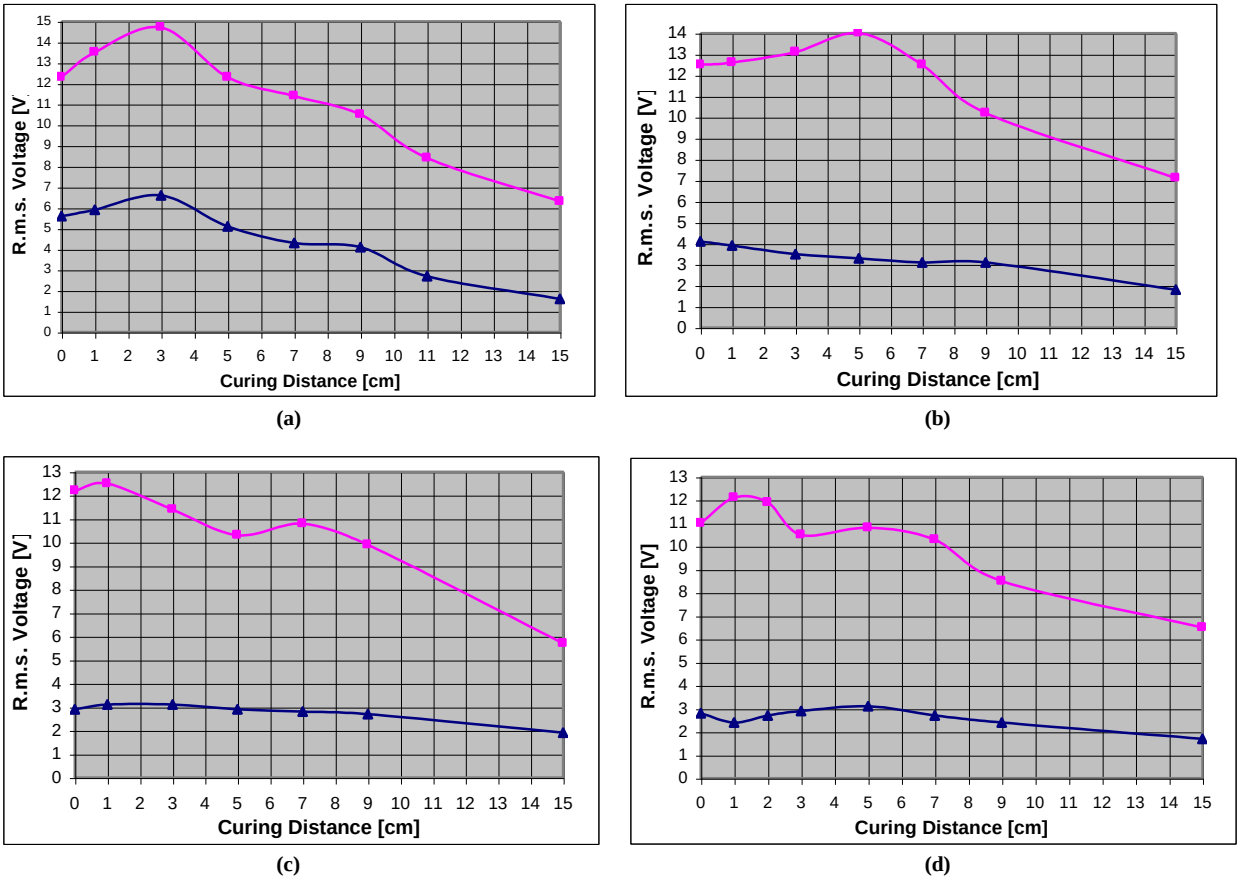

Graph 10: Values of V_{10} (triangles) and V_{90} (squares) for PDLCs cured at various distances, at 22° C, for **(a)** 48 w/w % LC, **(b)** 53 w/w % LC, **(c)** 60 w/w % LC, and **(d)** 65 w/w% LC, using a sine-wave of frequency of 1 kHz

Graphs 10(a) to **(d)** show that the switching voltages generally get larger as the curing distance decreases, except at small distances of curing where the voltages can be seen to drop. The close relationship between V_{10} and V_{90} implied by **(13)** only holds true for 48 w/w % LC; for other LC concentrations, V_{10} and V_{90} can be seen to exhibit contradictory trends. The general trend for V_{90} can be understood by considering that larger droplets should be conducive to smaller switching voltages, in agreement with **(13)**, due to their smaller surface-area-to-volume ratios, meaning that the LC molecules at the surface of a droplet exert far less influence on LC molecules in the interior, resulting in less anchoring energy and frictional forces opposing director reorientation. However, as droplets become larger, they are less mechanically stable, and are thus more likely to become deformed; this is exacerbated by the fact that the larger curing distances at which larger droplets are formed are also conducive to greater coalescence, fuelling even further droplet deformation. This extra anchoring energy should oppose director reorientation, leading to larger switching voltages, in agreement with **(13)**; for smaller curing distances, this is what is observed, but as the droplets get larger (i.e. as the curing distance increases), this energy starts to have less and less effect.

Graphs 10(a) to **(d)** also show that there is some truth in the claim[8] that higher LC concentrations lead to lower switching voltages, especially at small curing distances; this can be simply explained by knowing that larger LC concentrations are conducive to larger droplets, which manifest lower switching voltages especially at smaller curing distances due to the less significant impact of droplet deformation associated with high curing intensities.

Repeat measurements showed that the error on a value of switching voltage may be as much as ±1V, due to the placement of the PDLC in the path of the beam being critical. **Graph 11** shows how the largest source of error is not in the actual measurement of the voltages, but in the fabrication of the PDLCs. As already explained, the stated curing temperatures are only correct to the nearest 3° C, which can be seen to cause ±2 V deviations in the measured values of switching voltages, at around room temperature.

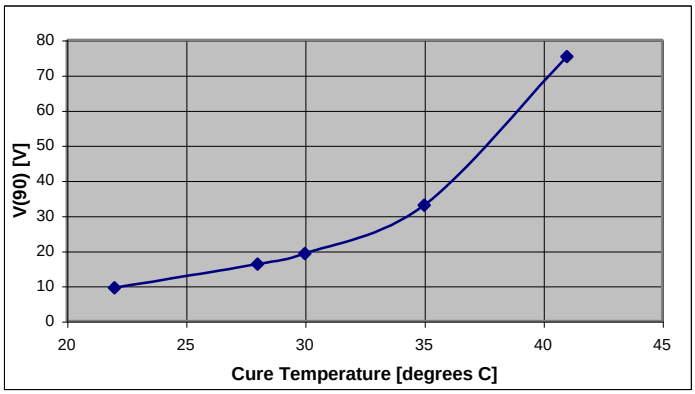

Graph 11: Evidence that the switching voltage is a strong function of the cure temperature, for a PDLC with 48 w/w % LC, cured at a distance of 9 cm

The enormous increase in switching voltage for larger temperatures of curing is unlikely to be solely due to a decrease in droplet size, since V_{10} shows no increase at all, even at the curing temperature of 41° C. Significant droplet deformation is not viable for very small droplets, due to the very large surface tension, so this can be ruled out as a culprit. An alternative explanation for the increased values of V_{90} is that the increased thermal energy of the LC molecules for high temperatures of curing allows a significant number to slightly burrow into the droplet walls, just prior to complete solidification of the monomer, leaving them permanently stuck in the polymer, but where they can still influence LC molecules that are free to move in the droplet; this scenario may not significantly impede slight director reorientation, but might provide dire consequences for attempts to fully switch the droplets, requiring enormous applied fields.

3.7 Experiment 5: Switching Speeds

3.7.1 Experimental Procedure

Expressions exist for the rise and decay times of a PDLC that explicitly relate them to droplet size and deformation; thus, measurements of these times for PDLCs prepared with a range of LC concentrations, curing distances, and curing temperatures, should provide definitive evidence of how these preparation conditions affect the morphology of the polymeric binder. Also, if PDLCs are to be used to display moving images, it is vital that the switching speeds are less than 100 ms.

The experimental set-up, depicted in **Fig.13**, can be seen to be similar to those in earlier experiments, only now the switching of the PDLC is controlled by a laptop computer, which also measures the photodetector response, via an assortment of electronics. The distance of 40 cm between the PDLC and the second lens has been retained, to yield the

maximum possible change in transmission between the ON and OFF states. The laptop was running a program that could control the frequency and magnitude of a square-wave voltage applied to the PDLC, up to 25 V_{p-p} (12.5 V_{rms}); the use of higher voltages, by using a step-up transformer, was deemed inappropriate, since this would distort the waveform leading to an unknown applied voltage. The program could display the photodetector voltage as a function of time, so that the time taken for the transmission to increase from 0 to 90% (i.e. the rise time), and the time taken for the transmission to decrease from 100 to 10% (i.e. the decay time), could be measured. The rise and decay times, at 25 V_{p-p} and 1 kHz, for PDLCs of varying LC concentration and distances of curing, were measured 10 times each so that error analysis could be performed. It is found[27] that the temperature of a PDLC can significantly affect its switching speeds, hence every attempt was made to ensure that, during measurements, all PDLCs were at the same temperature of 22° C.

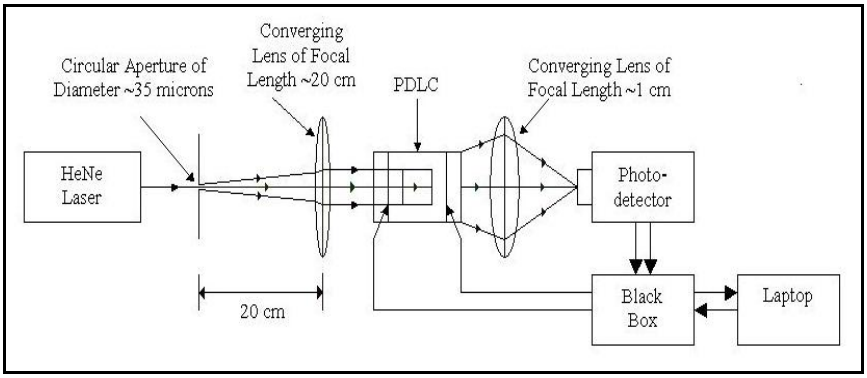

Fig.13: Scheme of the experimental set-up used for measurements of the switching speeds of PDLCs

It is predicted in **(15)** that spherical droplets have a rise time that is inversely proportional to the square of the applied electric field. To test this, voltages from 12.5 to 25 V_{p-p} (i.e. 6.25 to 12.5 V_{rms}), in small increments, were applied across the PDLC, for frequencies of 0.5, 5.5, and 10.5 kHz; this procedure was automated by the program on the laptop that also provided error analysis by taking repeat readings of every measurement. This data was achieved for PDLCs with LC concentrations of 48 and 65 w/w %, for various curing distances.

3.7.2 Results and Discussion

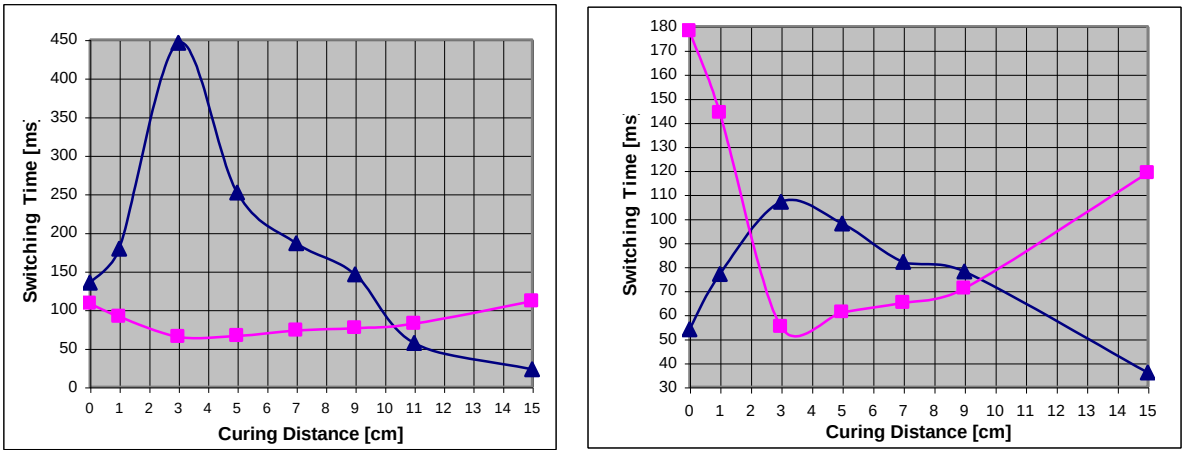

(a) **(b)**

Graph 12: Values of rise time (triangles) and decay time (squares) for PDLCs cured at various distances, at 22° C, for **(a)** 48 w/w % LC, **(b)** 53 w/w % LC, **(c)** 60 w/w % LC, and **(d)** 65 w/w% LC. The errors in the times were measured to be as much as ±5 ms, by calculating the standard error on the mean values

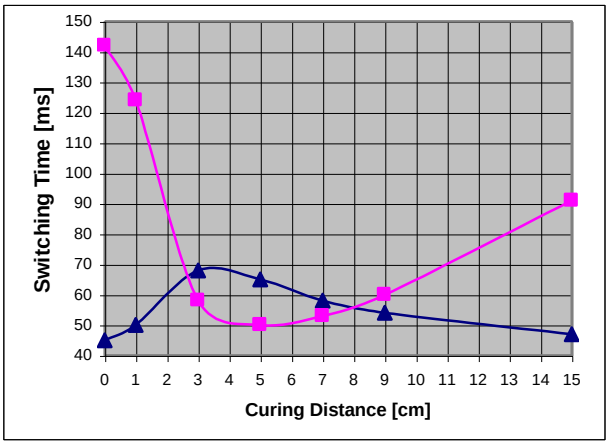

(c)

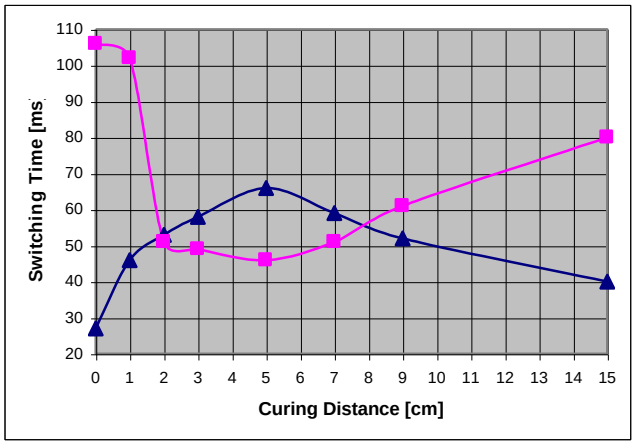

(d)

It can be seen from **Graph 10(a)** that the switching voltages for PDLCs with 48 w/w % LC, cured at 1 and 3 cm, are higher than the voltage used in the switching speed experiments (i.e. 12.5 V_{rms}). This explains why the rise times in **Graph 12(a)** are so high for the PDLCs cured at 1 and 3 cm; even though the droplet directors undergo less rotation for incomplete switching, the rotation still takes longer to perform. The corresponding decay times are then shorter, because the directors have less rotation to do to resume their original orientations. The same logic can be used to explain the rise and decay times observed in **Graph 12(b)**, at curing distances of 3 and 5 cm. Disregarding these results, it is apparent from **Graphs 12(a)** to **(d)** that smaller rise times are achieved by curing very close to the lamp, and these increase as the curing distances increase, up to a point, after which the rise times steadily decrease with increasing curing distance. This can be explained by considering that highly spherical droplets will be formed by curing very close to the lamp, due to the increased surface tension of smaller droplets, and because the fast rate of polymerisation provides little time for droplet coalescence, hence there is not much resistance in the form of anchoring energy opposing director reorientation; the increased effect of friction at the droplet surface for smaller droplets seems to have little effect. This is in agreement with **(14)**, which predicts that the effect of droplet size on the rise time is negligible for very spherical droplets. As the curing distance is increased, the droplets will become bigger and more deformed, and this can be seen to increase the rise times, up to a point, and then they see a continual decrease. This can only be explained if the effect of droplet deformation is dominant at small curing distances, increasing the rise times, up until the effect of increased droplet size becomes more influential, decreasing the rise times due to the decreasing effect of the LC molecules at the surface of the droplets. This is in direct conflict with **(14)**, which predicts that smaller, more deformed droplets are conducive to smaller rise times; this leads to the conclusion that the plus sign in the denominator of **(14)** should be a minus sign. **Graphs 12(a)** to **(d)** also show that PDLCs with higher LC concentrations are generally conducive to faster rise times, and this is simply by virtue of the increased droplet size.

For all distances of curing, it can be seen that an increased rise time leads to a decreased decay time. At small curing distances, the decay time can be seen to be very large, and this is easily explained if the droplets are highly spherical, since there is very little anchoring energy to cause the droplet directors to “spring back” to their original

orientations. As the curing distance is increased, the more pronounced droplet deformation leads to faster decay times, up to a point where the increased droplet size becomes more dominant, increasing the decay times; the droplet directors in larger droplets take longer to resume their original orientation because it is only LC molecules at the surface of a droplet that determine the director orientation, once the field has been removed. The effect is analogous to a domino rally, where the reorientation of the domino at the front of the queue leads to subsequent reorientation of all the dominoes in the line; the more dominoes there are in the line, the longer it takes for all to become reoriented. However, once the director has relaxed in a large droplet, it is more likely to have fully relaxed, due to the LC molecules at the surface of the droplet being more able to overcome the frictional forces, since they are aided in their reorientation by the thermal vibrations of a greater number of LC molecules, leading to the observed decrease in hysteresis. The observed decay times in **Graphs 12(a)** to **(d)** can be seen to be very well described by **(16)**. The finding that decreasing values of V_{10} and V_{90} are related to increasing values of decay time only for PDLCs with a low LC concentration[16] is not corroborated here. It is futile to observe how curing temperature affects the switching speeds of PDLCs, due to the associated increase in switching voltages.

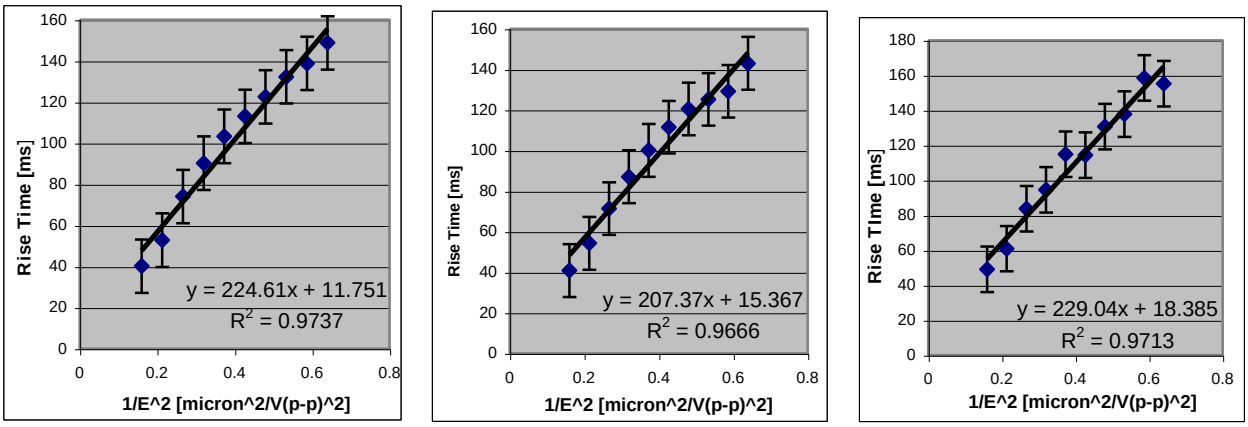

Graph 13: Validity test of **(15)**, showing how the rise time is inversely proportional to the square of the applied electric field, for a PDLC with 65 w/w % LC, cured at a distance of 15 cm, at 22° C, at a frequency of square wave of, **(a)** 0.5 kHz, **(b)** 5.5 kHz, and **(c)** 10.5 kHz. The gradient is the speed factor

Graphs 13(a) to **(c)** show that **(15)** is indeed valid, but only for applied voltages that are close to, or greater than, V_{90} of the PDLC. As the applied voltage gets much lower than V_{90}, the rise times no longer increase with decreasing applied fields, but actually start to *decrease*, when the effect of decreased droplet director reorientation becomes dominant; this leads to *negative* speed factors. This means that, from the perspective of **Graphs 10(a)** to **(d)**, reliable speed factor data could only be ascertained for PDLCs with low switching voltages (i.e. those cured at distances of at least 9 cm), since those with a large switching voltage yielded data with a linear regime spread only over 2 or 3 data points; decreasing the voltage increment, and taking data only over a small range at the highest voltage, was not found to yield reliable results. It is therefore not possible to make a meaningful comparison of the speed factors of PDLCs of different preparation conditions, suffice to say that it would be expected to decrease for PDLCs with smaller switching voltages, since then the magnitude of an applied field is likely to have less effect on the switching speed. A small speed

factor is highly desirable for PDLCs if they are to be used to display animated images, where it would not be ideal for the frame rate to be related to pixel opacity. It is apparent from **Graphs 13(a)** to **(c)** that the speed factor, and the rise time, are frequency dependent, and that frequencies of the order of 1 kHz are optimum; this dependence must arise, from **(14)**, by virtue of the frequency dependence of the dielectric constants of the LC and polymer, also causing the switching voltages to have a frequency dependence, from the perspective of **(13)**.

3.8 Fabrication of a Dye-Doped PDLC

The method for fabricating dye-doped PDLCs is very similar to that employed in the creation of undoped PDLCs, only now a small quantity of dye is mixed with the LC, prior to addition of the monomer. The empty plastic container was first weighed using high precision digital scales, and then the dye was carefully added, using a spatula, until the desired quantity was reached. Achieving a specified w/w % concentration of dye in the LC/monomer mixture is virtually impossible, since this relies on predicting what the masses of the LC and monomer quantities are going to be. It was important to try to place all the dye in the base of the container, since this is where it is to be eventually mixed with the LC; however, all the dyes, especially KD-184, were found to cling to the side of the container, causing problems later on. A magnetic spin bar was also placed in the container, since this was deemed to be the best means of stirring the dye/LC mixture. The cap was then placed on the container, before it was weighed once again.

Some of the dyes came in the form of clumped material, so it was ideal to mash these into a fine powder before the LC was added; this was achieved by placing the container on the stirrer for several minutes, so that the spin bar would grind down the dye on its base. The appropriate quantity of LC was then added to the container, in the glove-box, as detailed in §**3.2**. The container was then reweighed and sealed, as before. To combat the problem of the dye clinging to the interior wall, the container was placed in a centrifuging machine, upside-down, for several minutes; this sent all of the dye/LC mixture to the top of the container. The container was then centrifuged again, but this time the correct way up, bringing all the mixture back down into the base of the container, seemingly bringing all the dye particles down with it. A very small quantity of mixture was often found to remain in the cap, but this was deemed to have negligible consequences. The container was then placed in a beaker of shallow water, and placed on a hotplate/stirrer, where it was heated to close to 100° C, and spun for several hours. To ensure that as much dye was dissolved in the LC as possible, the LC container was then placed directly on the stirrer, on maximum power, and left for at least three days.

The monomer was then added, as previously described, and after being reweighed (with the omission of the sealing film), the container was then placed in the sonic bath for several hours. The mixture was now found to be too viscous to allow it to be mixed on the stirrer, unless the temperature was increased; this was done in a beaker of heated water, as before, but mixing in the sonic bath was found to produce equally good results, and was a simpler method.

Filling the cells was achieved as previously described, but for at least one of the dyes (namely KD-184) there existed a dependence of the colour of the finished cell on the temperature of filling, where filling at room temperature

gave only a lightly coloured cell (which did not always have a uniform texture after curing), but with a very transparent ON state. This suggested the presence of undissolved particles of dye in the mixture, and heating the cell allowed these micron-sized particles of dye to enter it, leading to a permanently coloured ON state. Removal of undissolved dye from the mixture, before filling cells, was thus highly desirable, but there exists no satisfactory way of doing this. Filtering of the mixture was deemed unviable, since this had the effect of removing the majority of the dye. Centrifuging the mixture caused the heaviest (i.e. undissolved) particles to germinate to the bottom of the container, but it was virtually impossible to scoop up mixture with the pipette spout *only* from the surface. Continually centrifuging the mixture, and removing the undissolved constituents each time, will probably eventually lead to removal of *all* the dye, since the van der Waals forces are not particularly strong; this method would also probably lead to an unknown LC concentration.

The only solution was to ascertain the solubility limit of the dye in the LC, but finding this limit, and staying below it, was very difficult. It was hoped that the extinction coefficients of the dyes, which were calculated earlier, could be used to ascertain the *actual* dye concentration in a PDLC cell, but the monomer's oxidising agents, and acidity, were found to severely impair the absorption of all the dyes. This is shown in **Table 4**, where the values of absorbance (corrected for the presence of the glass cell) of uncured PDLCs (of known concentration), could be used to predict the dye concentration, by using **(8)** with the values of the dye extinction coefficients given in **Table 2**; for all dyes, the predicted concentration is less than the actual concentration.

Dye	Pre-Cure Peak Absorption [arb. units]	Predicted Dye Concentration [molar]	Actual Dye Concentration in LC/Monomer [molar]
AK-00-41	0.524	0.00748	0.00851
KD-9	0.303	0.01943	0.03086
KD-10	0.153	0.01612	0.04699
KD-184	0.28	0.01317	0.03856

Table 4: Proof that the absorption of a dye is severely impaired when placed in NOA 65. The predicted concentration of dye in an uncured PDLC (calculated by using its absorbance, corrected for the presence of the glass cell) is considerably less than the actual concentration

In an attempt to increase the colour properties of a PDLC, it may be useful to cure the film with an electric or magnetic field parallel to the substrates; to provide a sufficiently large electric field across a distance of ~2 cm would require a dangerously large voltage, hence this is impractical. This meant that a magnetic field was the only viable option, but unfortunately a field as large as 1 Tesla was found to be completely unable to switch a PDLC.

3.9 Electro-Optical Properties of PDLCs Doped with AK-00-41

The extremely large extinction coefficient of AK-00-41 means that only a very small quantity of the dye is required to produce highly coloured displays. **Table 5** shows the electro-optical properties of just two cells, of different dye concentrations, where it is evident that the CRs are very small; this makes them unsuitable for PDLC applications.

Dye w/w %	LC w/w %	CR [arb. units]	OD CR [arb. units]	V10 [V(rms)]	V90 [V(rms)]	Rise Time [ms]	Decay Time [ms]
0.24	67	2.4	1.8	2.1	3.5	49	55
0.61	67	2.1	1.6	2.2	3.4	26	60

Table 5: Electro-optical properties of PDLCs doped with AK-00-41, cured at 5 cm, at 22° C

The low CRs are easily justified because of the dye's very low order parameter in BL001 (i.e. ~0.1), leading to a highly coloured ON state; the OD CRs were measured at the wavelength of peak absorbance, at 524 nm. The very low switching voltages may be explained by considering that the dielectric anisotropy of the LC mixture may have seen an increase, due to the dye molecules' alleged large dipoles, which may also explain the excellent rise times. The rotational viscosity of the mixture does not appear to have suffered any observable increase.

3.10 Electro-Optical Properties of PDLCs Doped with KD-8

Dye concentrations of 1, 1.5, and 2 w/w %, in ~50 w/w % LC, were found to produce extremely non-uniformly-cured PDLCs. This may be explained by considering how the dye was insoluble in methanol and acetonitrile - it is likely react with NOA 65 in an unusual way. Interestingly, using 2.5 w/w % dye, in ~50 w/w % LC, produced a reasonable light yellow PDLC, with a high OD CR of 4.6, at λ_{max}=387 nm, when cured at 5 cm, and 22° C. However, the OD CRs of PDLCs containing dyes with peaks of absorption at smaller wavelengths will be anomalously high, due to the increased scattering at these wavelengths. Also, it is a common observation that very weakly coloured cells (which is certainly the case here) have high OD CRs, due to the quantity depending more strongly on the ON state absorbance than the OFF state's. Also, contrary to expectations (due to the dye's measured high absorption at the wavelength of curing), the PDLC was found to fully polymerise in under 3 minutes, leading to a highly scattering cell analogous to an undoped PDLC; indeed its other electro-optical properties are similar to those of non-dye-doped PDLCs for the same preparation conditions. In conclusion, despite its high order parameter, KD-8 is unsuitable for use in PDLCs, not least because of its temperamental nature.

3.11 Electro-Optical Properties of PDLCs Doped with KD-9

Dye concentrations of up to 10 w/w % were attempted for this dye (as with all the dyes), but the best-coloured cells resulted for concentrations of around ~2 w/w %. Higher OD CRs result for slightly less-coloured cells, by using an even lower dye concentration. **Table 6** shows the properties of PDLCs doped with 0.9 w/w % LC, where an extremely high OD CR of 6.7, at λ_{max}=446 nm, has been achieved at 0 cm curing, probably by virtue of the smaller droplets producing greater scattering. All the electro-optical properties follow the trends observed for undoped PDLCs, except the decay time, whose trend is very difficult to explain. An attempt was made to achieve the same dye concentration in ~65 w/w % LC, but the closest managed was 0.4 w/w %, in 53 w/w % LC, which could only muster an OD CR of 4.

Cure Distance [cm]	CR [arb. units]	OD CR [arb. units]	V10 [V(rms)]	V90 [V(rms)]	Rise Time [ms]	Decay Time [ms]
0	4	6.7	3.3	10.6	45	176
1	3.1	4.4	2.1	7.9	32	227
2	2.9	4.1	2.1	7.7	26	281
5	2.5	3.7	2.6	6.0	23	199
9	1.8	2.7	2.1	5.5	18	161

Table 6: Electro-optical properties of PDLCs doped with KD-9, for 0.9 w/w % dye, 48 w/w % LC, and cured at a temperature of 18° C, for 2 minutes each

There are doubts over the photostability of KD-9 in UV light, since placement of a highly coloured PDLC under the UV lamp for 5 minutes, at 0 cm, was shown to have an adverse effect on its colour.

3.12 Electro-Optical Properties of PDLCs Doped with KD-10

Highly coloured PDLCs could be made with KD-10, but the ON state was also highly coloured, leading to low contrast ratios, λ_{max}=624 nm. **Table 6** shows the properties of PDLCs with 2.1 w/w % dye, in 49 w/w % LC, cured at various distances. It would be expected that 0 cm of curing would be the optimum curing distance, due to KD-10's high absorption in the UV region, but 5 cm appears to produce the highest CRs, at the expense of a higher switching voltage. To ensure complete curing, each cell had to be cured for 30 minutes; contrary to expectations, KD-10 has a very high photostability, since placing a highly coloured blue PDLC under the UV lamp for 5 minutes, at 0 cm, was found to produce no discernible colour change.

Cure Distance [cm]	CR [arb. units]	OD CR [arb. units]	V10 [V(rms)]	V90 [V(rms)]	Rise Time [ms]	Decay Time [ms]
2	1.6	1.9	2.3	8.6	14	281
3	2	3.1	2.0	11.5	23	187
5	2.2	4.1	2.7	13.1	38	120
9	2	3.39	2.2	8.1	39	202

Table 7: Electro-optical properties of PDLCs doped with KD-10, for 2.1 w/w % dye, 49 w/w % LC, and cured at a temperature of 18° C, for 30 minutes each

The data in **Table 7** is very difficult to explain, with counter-intuitive results. Extremely controlled conditions in the PDLC-fabrication process are clearly necessary in order to produce more conclusive results. An attempt was made to make a mixture with the same dye concentration, but with 67 w/w % LC, but the closest achieved was 1.5 w/w % in 57 w/w % LC, which could muster only an OD CR of 2.9, again at 5 cm of curing.

3.13 Electro-Optical Properties of PDLCs Doped with KD-184

Dye w/w %	LC w/w %	Cure Distance [cm]	CR [arb. units]	OD CR [arb. units]	V90 [V(rms)]	Rise Time [ms]	Decay Time [ms]
1.1	55	5	3.6	5.6	9.7	29	159
1.8	51	2	2.8	6.5	8.9	27	213
1.8	51	5	4	6.6	12.1	35	125
1.8	51	9	2.6	3.3	5.8	13	327
2.7	40	2	3.3	5.5	9.2	27	202
2.7	40	5	3.8	5.6	10.9	46	81
2.7	40	9	2.8	2.5	6.1	21	340

Table 8: Electro-optical properties of PDLCs doped with KD-184, for various dye and LC concentrations, cured at a temperature of 18° C, for 2 minutes each. V_{10} has been omitted for reasons of space

Table 8 shows that KD-184 is ideal for doping PDLCs with, due to the excellent electro-optical properties it can produce. 2.7 w/w % dye is found to produce the most highly coloured PDLCs, but this is at the expense of a more coloured ON state, leading to lower OD CRs. 1.8 w/w % dye in 51 w/w % LC is found to produce the best results, at a

curing distance of 5 cm, producing a PDLC with an OD CR of 6.6, at λ_{max}=520 nm. Further experimentation at smaller curing distances is clearly required, but a shortage of mixture prevented this; achieving the same dye concentration again is extremely difficult. An attempt was made to retain this dye concentration, but increase the LC concentration to ~65 w/w %, but the best achieved was 1.7 w/w % dye, in 59 w/w % LC, where the highest OD CR attained was only 4.4, at a curing distance of 5 cm. This suggests that either tiny changes in dye concentration make a profound difference to the finished PDLC, or that lower LC concentrations produce better PDLCs with this dye. Ascertaining how to achieve low switching voltages, whilst maintaining fast decay times, will clearly be a worthwhile avenue for possible future research.

The PDLCs with the highest values of OD CR for the dyes, KD-9, KD-10, and KD-184, are shown in **Appendix B**.

3.14 Experiment 6: Angle of Incidence Dependence

3.14.1 Experimental Procedure

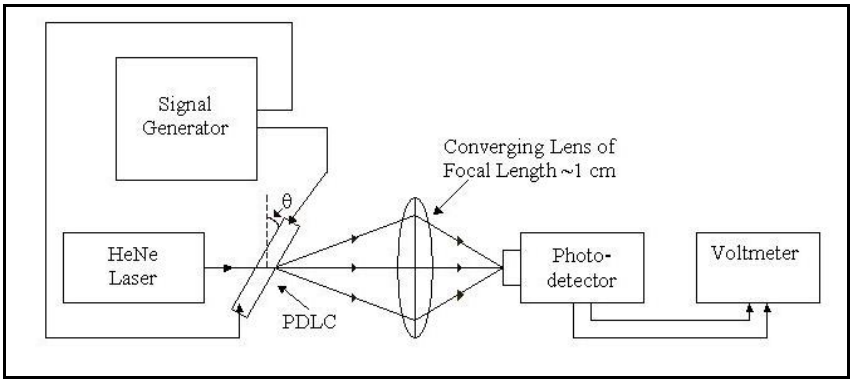

Fig.14: Plan view of the experimental set-up used to measure how the transmittance of a PDLC in the ON state is related to the angle of incidence of the probing light

In order to probe the effect of the extraordinary refractive index of a PDLC in the ON state, it is necessary to measure how well it transmits light at different angles of incidence. It is also of use to see the effect of doping with dyes on a PDLC's ON state, when viewing a cell at wide angles. To do this, the experimental set-up shown in **Fig.14** was used; the method of expanding the beam by using an aperture was now abandoned, since it is now necessary to illuminate the PDLC with as small a beam as possible, so that tilting the cell to wide angles, θ, still allows the entire cross-section of the beam to pass through the ITO. The distance from the PDLC to the lens was 40 cm, to thoroughly test the transparency of a PDLC's ON state. The cell containing cured NOA 65 was used to normalise the transmitted intensity, by measuring the photodetector voltage for different angles of tilt of the cell, from 0 to 85° (in increments of 5°), when placed to intercept the beam in the centre of the ITO. The translation of the beam upon passage through the cell will have no effect on the measured transmission due the large size of the receiving lens. PDLCs of concentration 65 w/w % LC, cured at distances of 3, 9, and 15 cm, at a temperature of 22° C, were tested in the same way as for the NOA 65 cell, as well as a cell containing KD-184, which has an OD CR of 5.5, with the cells in the ON state. The value of transmittance at a certain angle is then calculated by simply finding the ratio between the photodetector voltages corresponding to the transmitted intensities of the PDLC (in the ON state) and the NOA 65 cell, at that angle.

3.14.2 Results and Discussion

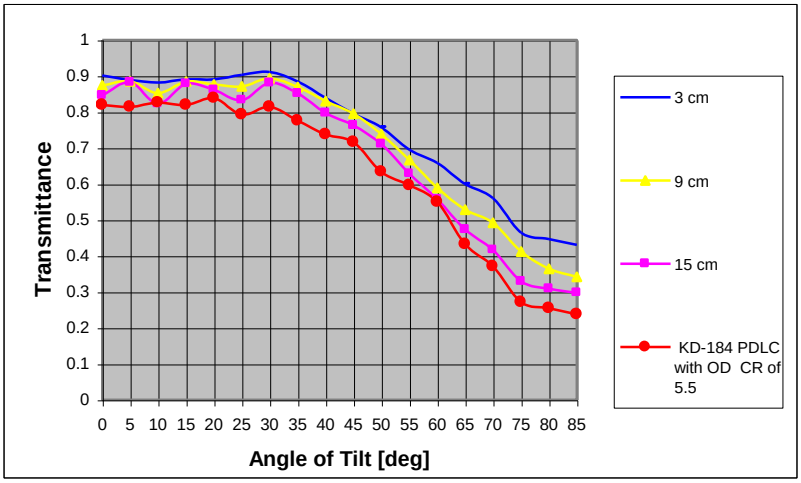

Graph 14: The viewing angle characteristics of PDLCs with 65 w/w % LC, with different curing distances, and a PDLC doped with KD-184 (with a high OD CR). PDLCs with smaller droplets can be seen to have marginally better viewing angle characteristics

Graph 14 shows that PDLCs with smaller droplets have a slightly better viewing angle characteristics; this result concurs with the data given in **Table 3**. This is contrary to what might be expected, and contravenes previous theoretical and experimental results.[6] It would be expected that larger droplets are conducive to a more transparent ON state, for the simple reason that the number density of droplets is lower, so there are fewer entities to scatter the light. However, the presence of greater deformities in larger droplets seems to lead to some droplets which do not switch fully with an applied field, and hence are able to cause a remnant of scattering in the ON state. These results are not entirely conclusive, but they do suggest that the models used to predict the light scattering from a PDLC in the ON state should consider the effects of droplet shape. The coloured PDLC, depicted in **Fig.15**, can be seen to have an ON state that is reasonably clear when viewed at angles out to 60°, which compares favourably with TN-LCDs.

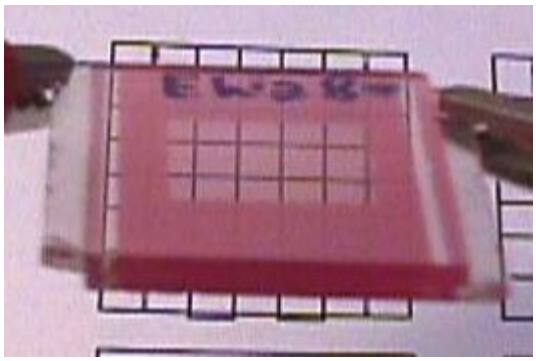

Fig.15: Photo of the PDLC whose viewing angle dependence is depicted in **Graph 14**, showing that the ON state is reasonably transparent, even when viewed at an angle of greater than 60°

3.15 The Creation of a Black Dye for PDLCs

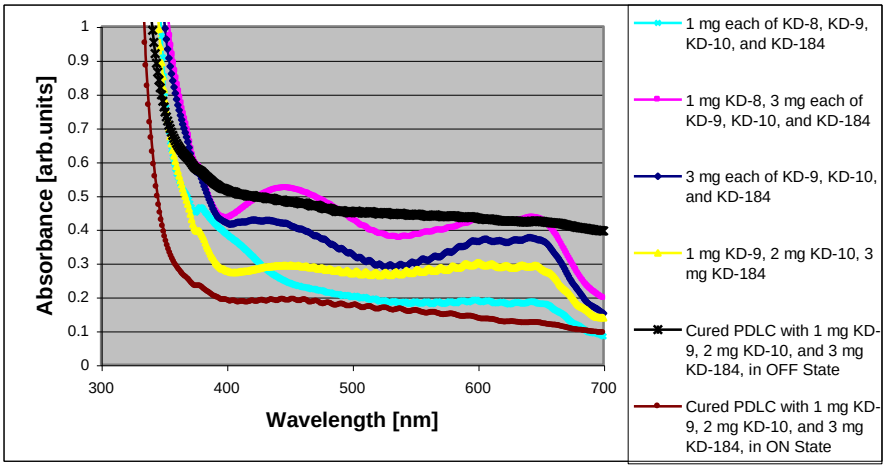

Graph 15: Absorption spectra of 4 uncured cells containing "black dyes" created by mixing the 4 Russian dyes together in different ratios. It is not the high absorption that is important, but the uniform absorption across the visible wavelengths. The best mixture was cured, and can be seen to give an OD CR of 2.8, at 550 nm. Approximately 100 µl BL001 and 100 µl NOA 65 were used in each mixture

If PDLCs are to be used for TV applications, they must be doped with a suitable black dye – using red/green/blue colour filters behind the PDLC could then possibly make a full-colour display. It has been reported[28] that a black dye can be created by combining the 4 Russian dyes in the correct proportions – unfortunately, the required ratios are not known. An accurate measurement of the LC concentration is not important here, so approximately 50 w/w % LC was used for each mixture. It was sensible to begin by using a 1:1:1:1 ratio, which can be seen in **Graph 15** to give too high an absorption at a wavelength close to KD-8's peak wavelength; hence, in the next mixture, larger quantities of the other dyes were used. This resulted in too much yellow, and slightly too much blue; given the temperamental nature of KD-8 in PDLCs, it was decided to attempt the same mixture, but with the omission of KD-8, which produced a similar result, showing that the inclusion of this dye was unnecessary. By using a 1:2:3 ratio of KD-9, 10, and 184, a dye exhibiting equal absorption at nearly all visible wavelengths was created. Upon curing at 5 cm, at 22° C, this cell was found to have an OD CR of 2.8, at 550 nm, which is reasonable; to increase this, larger dye quantities and higher LC concentrations (to lessen the detrimental effects of the monomer on the dyes' absorption) could be used, as well as a faster rate of curing. This "black" PDLC is shown in **Fig.16**.

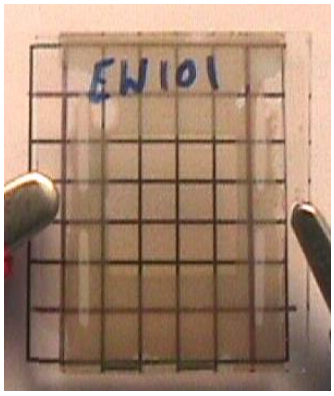

Fig.16: Photo of the best "black" PDLC created. The ON state can be seen to be very transparent, but the OFF state, whose appearance can be deduced by observation of the PDLC around the ITO, lacks opacity. This may be improved by a faster curing rate, using larger dye and LC concentrations, and increasing the thickness of the cell

Even if a dye could be created which appeared jet-black in a PDLC, there still exists the problem off curing the monomer in such an opaque cell. Very large droplets would result, which would lead to a very slow decay time and low scattering. The use of a cell gap of larger than 10 microns would also probably be necessary, leading to higher switching voltages.

3.16 Flexible PDLCs

Innovative Speciality Films (I.S.F.), Belgium, provided some flexible substrates that are 125 μm thick and coated with ITO. The presence of small particles of dust on the substrates prior to making a PDLC may be enough to cause visible imperfections in the finished film, hence the substrates had to be cut to the required size in a clean room, and handled with rubber gloves; transferring them to the glove-box involved wrapping the substrates in paper, to keep them meticulously clean. An attempt was made to fabricate flexible cells analogous to the prefabricated glass LC cells, by adhering the substrates together with epoxy resin, at a constant distance apart, using 9 μm spherical glass spacers (*Hirst Research*), so that the cells could be capillary-filled. However, such cells were found to be very brittle, and even slight

flexing was sufficient to cause the substrates to break apart; it was concluded that epoxy resin does not adhere to the ITO very well, so another means of keeping the substrates together had to be devised.

A successful attempt was made to weld the substrates together with NOA 65; a droplet of the monomer was placed on one of the substrates, and the other substrate was gently placed on top, without squeezing them together. After curing, this created a film that was about 40 μm thick (measured using Vernier callipers), and the 2 cm-long cell could be flexed by more than 1 cm at the centre before the polymer was observed to fracture; this level of flexibility was deemed more than adequate for the purposes of PDLCs, and the substrates took much coercion to pull apart. The creation of thinner films of cured NOA 65 was achieved by placing the glass spacers down the edges of the substrates, or by mixing the glass spacers in with the monomer, to result in films of thickness 9 μm; both types were found to fracture more easily than the thicker film.

Flexible PDLCs were then made using the three methods of fabrication used in making the NOA 65 films, using 48 and 65 w/w % LC concentrations. The 9 μm cells were more brittle, but had much better ON states than the thicker (~40 μm) cells. Upon light flexing, for the cells with 65 w/w % LC, it was observed that LC was moving around inside the polymer, showing that the polymeric wall between neighbouring droplets had broken down; the substrates separated quite easily once this had occurred. More success was achieved with the 48 w/w % LC cells, whose 2cm-long substrates could be flexed to about 0.5 cm before the polymeric wall was observed to break down, due to the decreased number density of droplets resulting in thicker walls between droplets. **Figs.17(a)** and **(b)** show the 48 w/w %, 9 μm (with the spacers mixed in with the mixture), flexible cell, which was found to have the best properties, in the ON and OFF states.

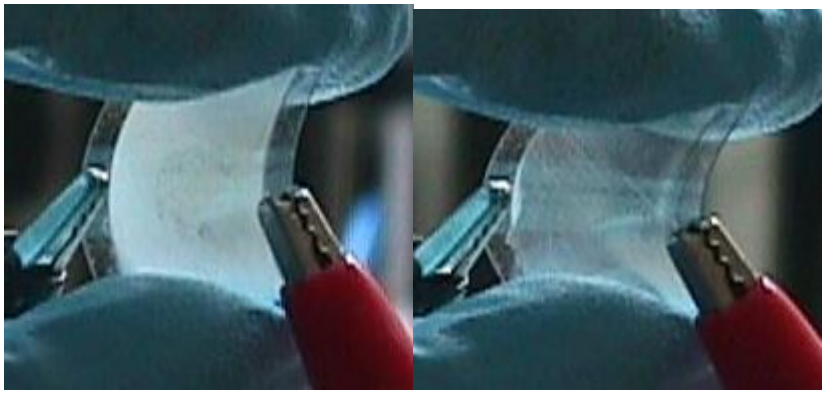

(a) **(b)**

Fig.17: Photos of the best flexible PDLC made, with 48 w/w % LC, and a cell spacing of 9 μm, in **(a)** the OFF state, and **(b)** the ON state, with a high degree of flexing. The imperfections in the ON state are a result of stirring the glass spacers into the mixture on the substrate

After several flexes, however, all flexible PDLCs were found to break apart. The crude method of filling the cell with mixture also leads to a non-uniform film. Hence, if a method of firmly adhering the substrates together at the edges could be fashioned, so that the cell could be capillary-filled, there is the possibility that fully useable flexible displays could become a reality, where they could be used in all manner of applications, such as being sewn into fabric to produce wearable displays! If the ultimate goal of finding a suitable black dye could achieved, there is the potentiality of creating “electronic paper” – a television in a display which is as light and flexible as a piece of paper!

4. FINAL CONCLUSIONS

PDLCs of various LC concentrations, curing distances, curing temperatures, and ultimately dye concentrations, have been fabricated, and it has been found that their electro-optical properties generally alter in a predictable way in response to these different preparation conditions. There exists no method of creating a PDLC where all the electro-optical properties are at an optimum level, since a high contrast ratio is usually at the expense of high switching voltages, large hysteresis, and a slow rise time. To some degree, the electro-optical properties can be tailored to suit a particular need, but highly controlled experimental conditions are required to do this, namely that the temperature of the curing process must be measured to supreme accuracy, and carefully regulated. Higher temperatures of curing almost invariably lead to a considerably higher switching voltage and impaired scattering. The effect of curing at lower temperatures needs to be examined, as there are suggestions that this leads to a lower switching voltage, greater scattering, and a lower absorption in the ON state of a dye-doped PDLC.

A reliable method of measuring the droplet size and shape is a prerequisite if further meaningful research is to be undertaken. The use of a more powerful optical microscope or, better still, an electron microscope, to image the LC domains, would elucidate considerable important information that was hidden in this work.

A more reliable method of measuring the contrast ratio is also urgently required, so that data is more reproducible, and can be compared with data of other workers, in different laboratories. The failure of the OD CR is that it is often PDLCs that are weakly coloured which have the highest values, even though they are visibly inferior; this stems from the sensitivity of the value to the ON-state absorption The spectrometer is much more sophisticated than the human eye at detecting the presence of colour, so what appears to be an uncoloured, transparent ON-state is often found to have a high absorption; this leads to the unfortunate situation that a qualitative description of a PDLC is sometimes better than a quantitative one. A contender for a better method of measuring the contrast ratio is based on the *reflection* of light from the PDLC, involving the use of an *integrating sphere*, which sadly could not be used in this work.

The use of LC cells with different cell gaps is another avenue of research worth pursuing, especially if highly opaque, black PDLCs are to be realised. It has been found to be possible to create a dye from 3 of the Niopik dyes that absorbs equally at nearly all visible wavelengths, but the opacity is very low. Increasing the dye concentration will only remedy this to a small degree; thicker cells are required, even though these will lead to an increase in switching voltages. This problem may be overcome if highly dipolar dyes, exhibiting high order parameters, could be acquired, but there is uncertainty over whether or not such dyes could possibly exist. The Niopik dyes clearly exhibit high order parameters, but there is no concrete evidence that they lead to faster rise times and lower switching voltages. PDLCs are not the ideal platform for making such deductions, since the addition of dye dopants often leads to an increased droplet size in PDLCs, which also has the effect of reducing the rise time and switching voltage.

The data obtained for the dye-doped PDLCs is not clear, and therein lies the problem with PDLC research. There are so many important parameters to be controlled that it is almost impossible to hold them all constant, and investigate the effects of a variation in just one of them. Using larger quantities of dye and LC per sample is the only way to eliminate the potentially huge errors involved in creating the mixtures. Though LC is very expensive, the costliest element of research is the pre-fabricated glass cells, of which several can be filled with the same mixture.

Hence, the use of flexible substrates appears to be a cheap and exciting alternative, but there are still several obstacles to be overcome; namely, a method of adhering the substrates to one another must be devised, as well as a solution to the problem of the polymeric wall breaking down or completely fracturing upon flexing. This has been partially addressed, by using smaller LC concentrations and making thicker films, but this will lead to an increase in switching voltages, and possibly a decrease in contrast ratio.

In conclusion, there still exist many exciting avenues of research in the field of PDLCs.

5. ACKNOWLEDGEMENTS

Many splendiferous folk and eminent scientists have aided and abetted me in my stroll down PDLC lane. Cornucopias of gracious thanks abound to my supervisors, Prof. “DB” Bloor, for his omniscience and Gandalf-like wisdom, and Dr. Lars-Olof Pålsson, for his unparalleled guidance, mirth, and tuition, not to mention his unrivalled Swedishness. A special mention must also go to scientist extraordinaire, and fellow 4th year research student, Mr. Andy Beales, who was an inspirational presence in the lab, and very kindly allowed me to use his order parameter data. Genius of Chemistry, Dr. Marek Szablewski, deserves plaudits aplenty for performing chemical wizardry on the dyes, and allowing me to use the results. Sony’s budding Einsteins, Akira Masutani and Tony Roberts, require special praise for their sage-like knowledge of PDLCs, and Tony for the use of his magnificent switching speed computer program. Luminaries of QTCs, Phil Hands and Dr. Kennyward Donnelly, deserve immense gratitude for their provision of light relief and enviable technical/laboratory/computer skills. All other members of the Optoelectronics Research Group are thanked immeasurably. The world’s greatest lab technicians, Wayne Dobby and Norman Thompson, deserve Knighthoods for their outstanding, tireless help and diligence. I.S.F. of Belgium are downright saintly for providing 2 sheets of their fabulous flexible substrates, free of charge. Finally, I would like to wish DB a long and blissfully happy *semi*-retirement.

6. REFERENCES

[1] C. Booth, P. Raynes, *Physics World (June),* **10**, 6, pp. 33-37, (1997)

[2] E. M. Korenic, *Optics and Photonics News (January)*, pp. 16-22, (2000)

[3] http://abalone.cwru.edu/tutorial/enhanced/files/LC/external/external.htm

[4] P. Kirsch, M. Bremer, *Angew. Chem. Int. Ed.*, **39**, pp. 4261-35, (2000)

[5] E. M. Terentjev, *Encyclopaedia of Materials Science and Technology*, Elsevier, pp. 4524-28, (2001)

[6] J. W. Doane, N. A. Vaz, B.-G. Wu, S. Zumer, *Appl. Phys. Lett.*, **48**, 4, pp. 269-71, (1986)

[7] S. J. Klosowicz, J. Zmija, *Optical Engineering*, **30**, 12, pp. 3440-50, (1995)

[8] I.-C. Khoo, S.-T. Wu, *Optics and Nonlinear Optics of Liquid Crystals (Vol. 1)*, pp. 221-9, World Scientific (1993)

[9] J. B. Whitehead Jr., S. Zumer, J. W. Doane, *J. Appl. Phys.*, **73**, 3, pp. 1057-65, (1993)

[10] G. P. Montgomery Jr., N. A. Vaz, *Applied Optics,* **26**, 4, pp. 738-43, (1987)

[11] G. H. Heilmeier, L. A. Zanone, *Appl. Phys. Lett.*, **13**, 3, pp. 91-2, (1968)

[12] S.-T. Wu, J. D. Margerum, M.-S. Ho, B. M. Fung, *Appl. Phys. Lett.*, **64**, 17, pp. 2191-93, (1994)

[13] J.-J. Wu, C.-M. Wang, W.-Y. Li, S.-H. Chen, *Jpn. J. Appl. Phys.*, **37**, 12A, pp. 6434-39, (1998)

[14] B. Bahadur, *Liquid Crystals - Applications and Uses (Vol. 3)*, p.71, World Scientific (1992)

[15] S. A. Carter, J. D. LeGrange, W. White, J. Boo, P. Wiltzius, *J. Appl. Phys.*, **81**, 9, pp. 5992-99, (1997)

[16] J. D. LeGrange, S. A. Carter, M. Fuentes, J. Boo, A. E. Freeny, W. Cleveland, T.M. Miller, *J. Appl. Phys.*, **81**, 9, pp. 5984-91, (1997)

[17] E. Shimada, T. Uchida, *Jpn. J. Appl. Phys.,* **31**, pp. 352-4, (1992)

[18] http://ising.phys.cwru.edu/proceedings/gsmith/gsmith.htm

[19] P. S. Drzaic, *Pure & Appl. Chem.*, **68**, 7, pp. 1435-40, (1996)

[20] C. R. Cantor, P. R. Schimmel, *Biophysical Chemistry Part II*, pp.812-3, W. H. Freeman and Co. (1980)

[21] B. S. Scheuble, *Kontakte, Merck (Part 1)*, pp. 34-48, (1989)

[22] Society of Liquid Crystal, *Dictionary of Liquid Crystal*, (1989)

[23] http://www.norlandprod.com/adhesives/noa65.html

[24] G. W. Smith, *Mol. Cryst. Liq. Cryst.,* **196**, pp. 89-102, (1991)

[25] N. A. Vaz, G. P. Montgomery, *J. Appl. Phys.*, **62**, pp. 3161-72, (1987)

[26] A. Beales, *Durham University M.Sci. Physics Research Project*, (2002)

[27] D. Coates, *Displays*, **14**, 2, pp.94-103, (1993)

[28] M. Olifierczuk, J. Zielinski, *Elsevier (Synthetic Metals)*, **109**, pp.223-7, (2000)

APPENDICES

APPENDIX A

The dyes which were found to be insoluble in BL001 are:

AK-00-20
AK-00-21
AK-00-22
AK-00-23
AK-00-28
AK-00-29
AK-00-30
AK-00-34
AK-00-35
AK-00-36
AK-00-37
AK-00-38
AK-00-39
AK-00-40
AK-00-42
AK-00-43

APPENDIX B

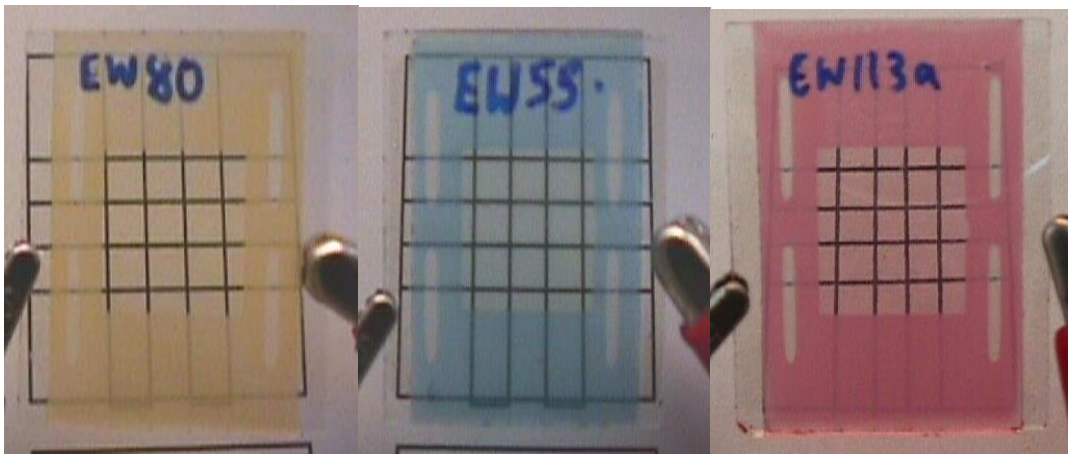

(a) **(b)** **(c)**

Photos of the PDLCs with the highest OD CR for **(a)** KD-9, **(b)** KD-10, and **(c)** KD-184. The PDLCs were held 1 cm above the grid surface